**RESEARCH REPORT**

EJN European Journal of Neuroscience  FENS  WILEY

# Nitric oxide increases gain in the ventral cochlear nucleus of guinea pigs with tinnitus

Adam Hockley[1,2,3] | Joel I. Berger[1,4] (iD) | Alan R. Palmer[1,5] | Mark N. Wallace[1,5] (iD)

[1]Medical Research Council Institute of Hearing Research, School of Medicine, University of Nottingham, Nottingham, UK

[2]School of Life Sciences, University of Nottingham, Nottingham, UK

[3]Department of Otolaryngology, Kresge Hearing Research Institute, University of Michigan, Ann Arbor, MI, USA

[4]Department of Neurosurgery, University of Iowa, Iowa City, IA, USA

[5]Hearing Sciences, School of Medicine, University of Nottingham, Nottingham, UK

**Correspondence**
Mark N. Wallace, Hearing Sciences, School of Medicine, University of Nottingham, Building 40, Nottingham, NG7 2RD, UK.
Email: mark.wallace@nottingham.ac.uk

**Abstract**

Previous work has led to the hypothesis that, during the production of noise-induced tinnitus, higher levels of nitric oxide (NO), in the ventral cochlear nucleus (VCN), increase the gain applied to a reduced input from the cochlea. To test this hypothesis, we noise-exposed 26 guinea pigs, identified evidence of tinnitus in 12 of them and then compared the effects of an iontophoretically applied NO donor or production inhibitor on VCN single unit activity. We confirmed that the mean driven firing rate for the tinnitus and control groups was the same while it had fallen in the non-tinnitus group. By contrast, the mean spontaneous rate had increased for the tinnitus group relative to the control group, while it remained the same for the non-tinnitus group. A greater proportion of units responded to exogenously applied NO in the tinnitus (56%) and non-tinnitus groups (71%) than a control population (24%). In the tinnitus group, endogenous NO facilitated the driven firing rate in 37% (7/19) of neurons and appeared to bring the mean driven rate back up to control levels by a mechanism involving N-methyl-D-aspartic acid (NMDA) receptors. By contrast, in the non-tinnitus group, endogenous NO only facilitated the driven firing rate in 5% (1/22) of neurons and there was no facilitation of driven rate in the control group. The effects of endogenous NO on spontaneous activity were unclear. These results suggest that NO is involved in increasing the gain applied to driven activity, but other factors are also involved in the increase in spontaneous activity.

**KEYWORDS**

auditory system, noise exposure, spontaneous activity, synaptic plasticity

# 1 | INTRODUCTION

Tinnitus is characterised by the perception of sound, independent of external stimuli. Synaptic plasticity producing gain increases in the central auditory system has been suggested to underlie some forms of tinnitus (Eggermont, 2015; Noreña, 2011; Shore & Wu, 2019). The location and mechanism of this central gain increase is complicated and probably involves multiple levels of the auditory system all the way up to the auditory cortex (Eggermont & Roberts, 2015; Shore, Roberts, & Langguth, 2016). Homeostatic plasticity involves neuromodulation facilitating or suppressing the strength of synaptic transmission to stabilise activity (Turrigiano, 1999), and has been suggested as a mechanism that could mediate central gain (Auerbach et al., 2014; Schaette & McAlpine, 2011; Sheppard, Liu, Ding, & Salvi, 2018). One of the neuromodulators prominently involved in synaptic plasticity is NO (Prast & Philippu, 2001), an intercellular messenger that can operate both in very localised signalling and as a volume transmitter (Hollas, Ben Aissa, Lee, Gordon-Blake, & Thatcher, 2019; Steinert et al., 2011). The enzyme synthesising NO exists in three main forms, but it is the neuronal form that is mainly relevant to this study. NO is involved in both long-term potentiation and long-term depression depending on the circumstances of its release and its site of action (Garthwaite, 2019). The localised signalling sometimes involves a postsynaptic complex where its synthesising enzyme neuronal NO synthase (nNOS) is bound directly to N-methyl-D-aspartate (NMDA) receptors (Christopherson, Hillier, Lim, & Bredt, 1999; Olthof-Bakker, Gartside, & Rees, 2019). This means that the calcium entering through the NMDA channels is directly available for activating the calcium-dependent, neuronal form of NOS.

The ventral cochlear nucleus (VCN) is one of the first nuclei in the auditory pathway, receiving most of its input from the auditory nerve, and it is thought to have a role in the development of tinnitus (Gu, Herrmann, Levine, & Melcher, 2012). It contains relatively high levels of neuronal nitric oxide synthase (Vincent & Kimura, 1992; Zheng, Seung Lee, Smith, & Darlington, 2006), the enzyme responsible for NO synthesis in a calcium-dependent manner (Knowles & Moncada, 1994). Changes to peripheral afferent input have been shown to alter nNOS levels in the auditory system. Cochleostomy, resulting in hugely decreased input, produces decreased spontaneous firing rates (Koerber, Pfeiffer, Warr, & Kiang, 1966) and increased nNOS expression in the VCN. This increase in nNOS may be associated with a redistribution of nNOS from a primarily cytoplasmic to a mainly membranous location where it is bound to NMDA channels (Chen, Huang, Wang, & Chen, 2004). Other less traumatic procedures that are accepted methods of inducing tinnitus, such as acoustic over-exposure (AOE; Alvarado et al., 2016; Coomber et al., 2014) and salicylate administration (Zheng et al., 2006), also resulted in increased expression of nNOS in the VCN, although not such a radical redistribution of its location.

Unilateral AOE produces neural changes that are mainly present in the ipsilateral CN (Dong, Mulders, Rodger, & Robertson, 2009; Dong, Mulders, Rodger, Woo, & Robertson, 2010), but this can also affect activity in the contralateral CN (Sumner, Tucci, & Shore, 2005), due to commissural connections at the CN level of the auditory brainstem (Schofield & Cant, 1996). Increases in the relative amount of nNOS occur after AOE in the ipsilateral VCN compared with the contralateral VCN, and this correlates with behavioural evidence of tinnitus (Coomber et al., 2014). We have postulated that changes to NO function may contribute to the amount of gain applied to neurons in the VCN and contribute to the development of tinnitus (Coomber, Kowalkowski, Berger, Palmer, & Wallace, 2015). nNOS is present in all the principal neuronal types of the VCN, and recent physiological work has provided some insight into the complicated role of NO in the undamaged VCN. Work using slices of mouse cochlear nucleus (Cao, Lin, Sugden, Connors, & Oertel, 2019) has shown that there is a network of T-stellate (chopper) neurons that are interconnected by interneurons in a reciprocal fashion. Both the input and output synapses of these interneurons are modulated by NO levels. There is also evidence from the guinea pig that in vivo, the firing rate of other principal neurons including onset cells (large stellate) and bushy cells (primary-like) is modulated by NO (Hockley, Berger, Smith, Palmer, & Wallace, 2020).

The present study used in vivo extracellular recordings in noise-exposed animals to examine the changes within the VCN and to correlate these changes with behavioural evidence of tinnitus. Iontophoresis was combined with these recordings to determine the physiological role of NO in the VCN following the development of tinnitus. This allowed us to test the hypothesis that the increases in NO production are responsible for maintaining driven firing rates at a normal healthy level despite the reduced afferent input associated with hearing loss in the tinnitus animals. In addition to increasing the driven firing rate, the elevated NO may also increase the spontaneous firing rate and lead to the perception of tinnitus. This hypothesis leads to a series of testable predictions:

1. Spontaneous firing rates will be increased in animals with tinnitus (T), but not in those that do not have tinnitus (NT)
2. Driven firing rate in T animals will be equal to control animals and greater than in the NT animals

3. The sensitivity to exogenous NO among neurons of the T animals will be different compared with the control or NT groups

4. Blocking endogenous NO production will reduce the driven firing rate of more neurons in the T group than in the control and NT groups.

5. If NMDA channels are involved in mediating the increased firing rates of T animals, then blocking endogenous NO production should reduce the effect of NMDA application, as it does in some neurons of the cat visual cortex (Cudeiro et al., 1997), rather than increasing the NMDA response, which is its more common action.

## 2 | MATERIALS AND METHODS

All animal experimental procedures were in accordance with the Animals (Scientific Procedures) Act 1986 and the European Communities Council Directive 1986 (86/609/EEC) following the approval of the Animal Welfare and Ethical Review Body at the University of Nottingham, UK.

### 2.1 | Animals

Male ($n = 11$) and female ($n = 15$) tricolour guinea pigs weighing 430–950 g at the time of noise exposure (approximately 2–9 months old during data collection) were used. Guinea pigs were bred in-house and group-housed on a 12/12-hr light–dark cycle, with food and water ad libitum.

### 2.2 | Tinnitus induction and behavioural confirmation

Animals were divided into two groups—noise-exposed non-tinnitus (NT); and noise-exposed tinnitus (T). Results from a third group of control (C) animals, which had not been noise exposed and did not undergo behavioural testing, were also available. Although being part of the same study, these results have been reported separately (Hockley et al., 2020). Both groups of noise-exposed animals underwent baseline testing for gap prepulse inhibition of acoustic startle (GPIAS), before acoustic over-exposure (AOE), followed by GPIAS testing at weeks 7–9 post-AOE. Animals that showed a significantly reduced GPIAS (see below) were classified as noise-exposed tinnitus.

Noise exposure was conducted as previously described (Berger et al., 2018). Anaesthesia was induced with ketamine (50 mg/kg, i.p.) and xylazine (10 mg/kg, i.p.), which was further supplemented when required with administrations of a ketamine and xylazine mix (15:2; i.m.). Core body temperature was monitored and maintained at 38 ± 0.5°C with a homeothermic heating pad (Harvard Apparatus Ltd.) attached to a rectal probe. Auditory stimuli were presented by loud speakers (Peerless DX25) connected to polyethylene tubes (20 mm diameter), which formed a seal around the ear. Calibration was performed using a 40BP 0.25-inch pressure condenser microphone and 26AC pre-amplifier (both G.R.A.S.) attached to a calibrated 1-mm-diameter probe positioned as close as possible to the entrance of the ear canal.

Using this set-up, the left ear was exposed to a band-passed noise (centre frequency 9 kHz; bandwidth 2 kHz), presented at 110 dB SPL for 1 hr. During this time, the right pinna was folded over and surrounded with a polyethylene tube plugged with cotton wool, in order to ensure that only the left ear was exposed. Guinea pigs remained inside a sound-attenuating booth for the duration of the noise exposure and auditory recordings. Auditory brainstem responses (ABRs) were recorded bilaterally with subcutaneous electrodes at the vertex and mastoids, before and immediately after AOE, to determine changes in hearing thresholds. Responses were recorded to pure tone pips (5 ms long with 1 ms on/off ramp) of between 5 and 20 kHz presented to the left ear using software written in MATLAB. Signals were processed with Tucker–Davis Technologies amplifiers RA4LI, RA16PA and System 3 interface RX7. Signals were filtered between 0.1 and 5 kHz and were averaged across 500 presentations where 50% of trials were phase-inverted. ABR measurements were usually repeated at the end point of the experiment, immediately before the surgery required for recording from the cochlear nucleus. In two instances, the middle ear was exposed instead via the bulla and a small silver ball electrode placed on the round window so that the compound action potential (CAP) could be recorded before the cochlear nucleus recordings were made. Pure tones (30 ms long, 1 ms ramps on/off) were presented in one octave steps between 0.5 and 16 kHz and in 5 dB SPL steps between 45 and 95 dB SPL, with a repeat period of 100 ms. CAP signals were filtered between 0.3 and 12 kHz. The root mean square (RMS) of the CAP response to each frequency-level combination was averaged across 10 stimulus repeats.

We identified animals as noise-exposed tinnitus (T) based upon the most commonly used behavioural model, gap prepulse inhibition of acoustic startle (GPIAS), that relies on measuring an innate reflex response to a startling stimulus. Briefly, the magnitude of the acoustic startle reflex evoked by a loud sound is reduced when the startling sound is preceded by a gap in an otherwise continuous background noise. This is known as gap prepulse inhibition (Berger, Coomber, Shackleton, Palmer, & Wallace, 2013; Turner et al., 2006). The impairment of gap detection (leading to reduced gap prepulse inhibition) observed following AOE was suggested to be caused by tinnitus "filling in" the gap, thus reducing its salience (Berger et al., 2013; Chen et al., 2013; Coomber et al., 2015; Dehmel, Eisinger, & Shore, 2012; Longenecker

& Galazyuk, 2011; Turner, Larsen, Hughes, Moechars, & Shore, 2012; Turner & Parrish, 2008). Others have suggested that the behavioural deficits may actually reflect a deficit in temporal processing associated with the AOE, rather than tinnitus per se (Chen et al., 2013; Fournier & Hebert, 2013). In our hands, at least, the deficits in gap prepulse inhibition seem to be associated with histological and physiological changes that are likely associated with tinnitus (Berger, Coomber, Wallace, & Palmer, 2016; Berger, Coomber, Wells, Wallace, & Palmer, 2014; Berger et al., 2018; Coomber et al., 2014, 2015). The GPIAS method relies on animals being able to detect a gap in the background noise presented before the startle stimulus. We have shown previously (Coomber et al., 2014) that auditory thresholds are initially elevated by the noise exposure and only partially recover over the 7–9 weeks during which tinnitus develops. However, the sound levels for GPIAS testing were carefully selected (Berger et al., 2018) so that this permanent threshold shift did not confound the estimates of GPIAS. The startle pulse was presented in free field, and as the AOE was only in the left ear, the hearing in the right ear remained within the control range.

We used a motion-tracking camera system (Vicon Motion Systems), consisting of three infrared cameras, to monitor flexion of the pinna, or the Preyer reflex. Reflective markers (4 mm diameter) were attached to the pinnae using cyanoacrylate adhesive. The motion-tracking system used these markers to triangulate the position of the ears and subsequently track three-dimensional pinna movement during the presentation of startling stimuli. Marker positions were recorded at a sampling rate of 200 Hz using Vicon Workspace software, and after each trial, raw data were exported to MATLAB® (R2009b) for analysis. From these measurements, the absolute positions and Euclidean distance of the markers were calculated and the magnitude of the Preyer reflex was expressed as pinna displacement (change in distance between right and left pinnae). By measuring flexion of the pinna, the resulting gap prepulse inhibition can be quantified (see Berger et al., 2013, for full details of the methods used).

## 2.3 | Surgery

Following the cessation of behavioural testing, guinea pigs were anaesthetised with 20% w/v urethane (4.5 ml/kg i.p.; Sigma) and Hypnorm solution (fentanyl/fluanisone; 0.2 ml i.m.). Further injections of Hypnorm of up to 0.2 ml i.m. were applied when required to maintain surgical anaesthesia. Artificial respiration with 100% oxygen and a pump rate of 100 cycles per min. was used to maintain normal end-tidal $CO_2$ partial pressure within a range of 28–38 mm of mercury. Core body temperature was maintained at $38 \pm 0.5°C$. Animals were placed in a stereotaxic frame within a sound-attenuating and electrically shielded chamber. Hollow

speculae replaced the ear bars and allowed direct vision of the tympanic membrane. The skull was exposed and levelled between 5 and 13 mm anterior to ear bar zero. A midline incision was made, the temporal muscle was removed, and a craniotomy was performed above the cerebellum from 1 to 5 mm lateral of midline to allow access to the left cochlear nucleus. The dura mater was removed, and the exposed brain surface was kept moist by regular application of warm saline or a layer of agar (1.5% solution in 0.9% saline).

## 2.4 | Sound presentation

Experiments were carried out in a sound-attenuating booth. Auditory stimuli were delivered monaurally via a closed-field system (modified Radioshack 40-1377 tweeters; M. Ravicz, Eaton Peabody Laboratory) coupled to damped 4-mm-diameter probe tubes, which fitted into the hollow earbars. The speakers were driven by a Tucker–Davis Technologies (TDT) System 3 module (RZ2), controlled by Brainware (software developed by J. Schnupp, University of Oxford, UK). A probe tube microphone (Brűel and Kjaer 4134 with a calibrated 1-mm probe tube) was used to calibrate the sound system close to the tympanic membrane. The sound system response was flat to within $\pm 10$ dB from 100 to 35,000 Hz (see Palmer & Shackleton, 2009, for an example calibration curve).

## 2.5 | Iontophoresis and extracellular recording

As previously described (Hockley et al., 2020), extracellular drug application was achieved using five-barrelled glass micropipettes (5B120F-4; World Precision Instruments (WPI)). Glass-coated tungsten recording electrodes with a tip length of 10 μm were made in-house (Bullock, Palmer, & Rees, 1988) and glued to the micropipette using 5-min epoxy resin. The drug barrels were filled with either the NOS inhibitor Nω-nitro-L-arginine methyl ester hydrochloride (L-NAME, 50 mM, pH 6.5), the NO donor 3-morpholinosydnonimine hydrochloride (SIN-1, 40 mM, pH 4.5), N-methyl-D-aspartic acid (NMDA, 10 mM, pH 8) or glutamate (100 mM, pH 8); all obtained from Sigma. The central barrel was filled with 2 M NaCl solution, to allow current balancing. Retaining currents of 10 nA were applied to drug barrels between ejections, with polarity opposite to the charge of the drug to be ejected. Retaining currents were positive for NMDA and glutamate and negative for L-NAME and SIN-1. Two barrels were often filled with the same drug so that if one started to block, the other could still be used. Cycling was used to maintain drug concentrations at the electrode tip between recordings, where

each drug barrel would be supplied with the ejection current for 8 s every 36 s. We never used L-NAME and SIN-1 in the same electrode assemblies, to avoid any interference between the drugs, due to leakage. All currents were applied by a Neurophore BH-2 (Digitimer) iontophoresis system consisting of four IP-2 iontophoretic pump modules and one BM-2 control and balance module.

The single-channel recording electrode was connected through an HS-2 headstage (×1 L; Axon Instruments Inc.) and an Axoprobe-1A microelectrode amplifier (×100; Axon Instruments Inc.), then further amplified x100 (IHR 4 Channel Amplifier). The resulting signal then passed to a TDT System 3, RZ2 processor for filtering (0.3–3 kHz), and online data collection was facilitated by Brainware at a sampling rate of 25 kHz. Spikes were detected online in Brainware by an arbitrarily set threshold, never less than double the peak-to-peak amplitude of the background noise to keep the risk of false positives at less than 5%.

Electrodes were advanced through the cerebellum to the left cochlear nucleus at a 45° angle using a Burleigh Inchworm (Burleigh Instruments). The VCN was located stereotaxically, often found 3.5–4.5 mm lateral of midline, ±1 mm anterior/posterior of ear bar zero, and 0–2 mm dorsal of ear bar zero. To test that the electrode assembly was working properly, ejection currents were applied to the glutamate barrel, while the electrode tip was within the cerebellum.

Upon isolation of a single unit in VCN, the frequency at the minimum threshold was determined (characteristic frequency, CF), and then, the unit was classified into one of five subgroups: primary-like (Pr), chopper (Ch), phase-locked (Ph), onset (On) or unclassified (Un) based on PSTHs formed from the responses to 50-ms CF tones at 20 dB suprathreshold as described previously (Hockley et al., 2020).

Over the next hour, pure tone pulse trains were presented continuously at the CF (200-ms tone pip, 800 ms silence, 3,600 repeats, 20 dB suprathreshold). Spike timings were recorded throughout the sweep, allowing offline analysis of the auditory-driven firing rate (initial 200 ms) or spontaneous firing rate (final 700 ms).

## 2.6 | Drug ejection periods and statistical analysis

Drug ejection periods and statistical analysis of changes to firing rate were as previously described (Hockley et al., 2020). Drugs were applied iontophoretically for different periods throughout the recording, and the spike rates before, during and after drug application were statistically compared with a Kruskal–Wallis test with Dunn's multiple comparison test.

SIN-1 was applied in 10-min epochs, on three occasions over an hour, using increasing ejection currents of 40, 80
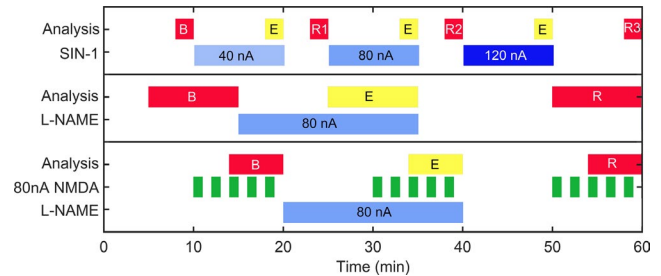


**FIGURE 1** The regime of drug applications (upper lines of each panel) and response measurements (labelled "Analysis"). For the statistical analysis, ejection: E blocks show periods in which the response to the drugs were measured, baseline: B blocks show baseline measurement periods and those labelled (R) show recovery periods

and 120 nA at 10–20, 25–35 and 40–50 min, respectively (Figure 1). Spike rates were computed in 10-s periods at the following time points: the final 2 min of baseline prior to drug ejection (baseline: B), the final 2 min during each drug ejection (ejection: E) and the final 2 min of each recovery period (recovery: R1, R2 and R3). In chronological order, the seven analysis periods were as follows: B, E at 40 nA; R1, E at 80 nA; R2, E at 120 nA; and R3. Analysis periods were compared using a Kruskal–Wallis test with Dunn's multiple comparison test, and responses were deemed significant if there was a significant change from R1 to 80 nA and R2 to 120 nA in the same direction, and a significant return towards baseline from 120 nA to R3.

L-NAME was applied at 80 nA for 20 min (from 15 to 35 min) during an hour-long recording (Figure 1). Spike rates were measured over 60-s periods, and the final 10 min of drug ejection (ejection: E) was compared with both the final 10 min of baseline (B) and the final 10 min of the recovery (R) using a Kruskal–Wallis test with Dunn's multiple comparison test. If both comparisons showed a significant increase during the E period, then the drug was deemed to have had a real effect.

The effect of L-NAME on NMDA-mediated excitation was measured during a 1-hr-long series of tone pulse trains. NMDA was applied at 80 nA for 1 min every 2 min between 10 and 20 min, 30 and 40 min, and 50 and 60 min, while L-NAME was applied at 80 nA from 20 to 40 min (Figure 1). This gave one baseline period of NMDA responses (B), one period of responses in the presence of L-NAME (E) and one recovery period (R). With these data in 10-s bins, the six bins with highest spike rate from the final three NMDA applications of each period were used. The baseline firing rate (mean of 180 s before the initial NMDA application of that period) was used to calculate the percentage change in firing rate evoked by NMDA. These increases for each period were compared using a Kruskal–Wallis test with Dunn's multiple comparison test.

# 3 | RESULTS

## 3.1 | Assessment of hearing loss due to noise exposure

Unilateral noise was presented to the left ear of 26 male and female guinea pigs for a total of 1 hr at 110 dB SPL. The presented sound was continuously monitored by a probe tube close to the pinna to confirm that the narrow-band noise was restricted to frequencies of 8–10 kHz (Figure 2a). The degree of hearing loss was assessed by comparing ABRs recorded before, immediately after and

~10 weeks after the AOE. An example of ABRs recorded in response to a 10-kHz sound pulse before and immediately after AOE is shown in Figure 2d where the dotted lines indicate the measurement window where results were analysed starting at 3 ms after the start of the sound pulse. These measurements were made automatically with the MATLAB software. The difference between the trough and peak of waves three and four within this window was plotted against pulse sound level for five frequencies as shown in Figure 2e–i. The amplitude of the ABR increases monotonically with increasing sound level, and the threshold was taken to be the point where the slope levelled out,
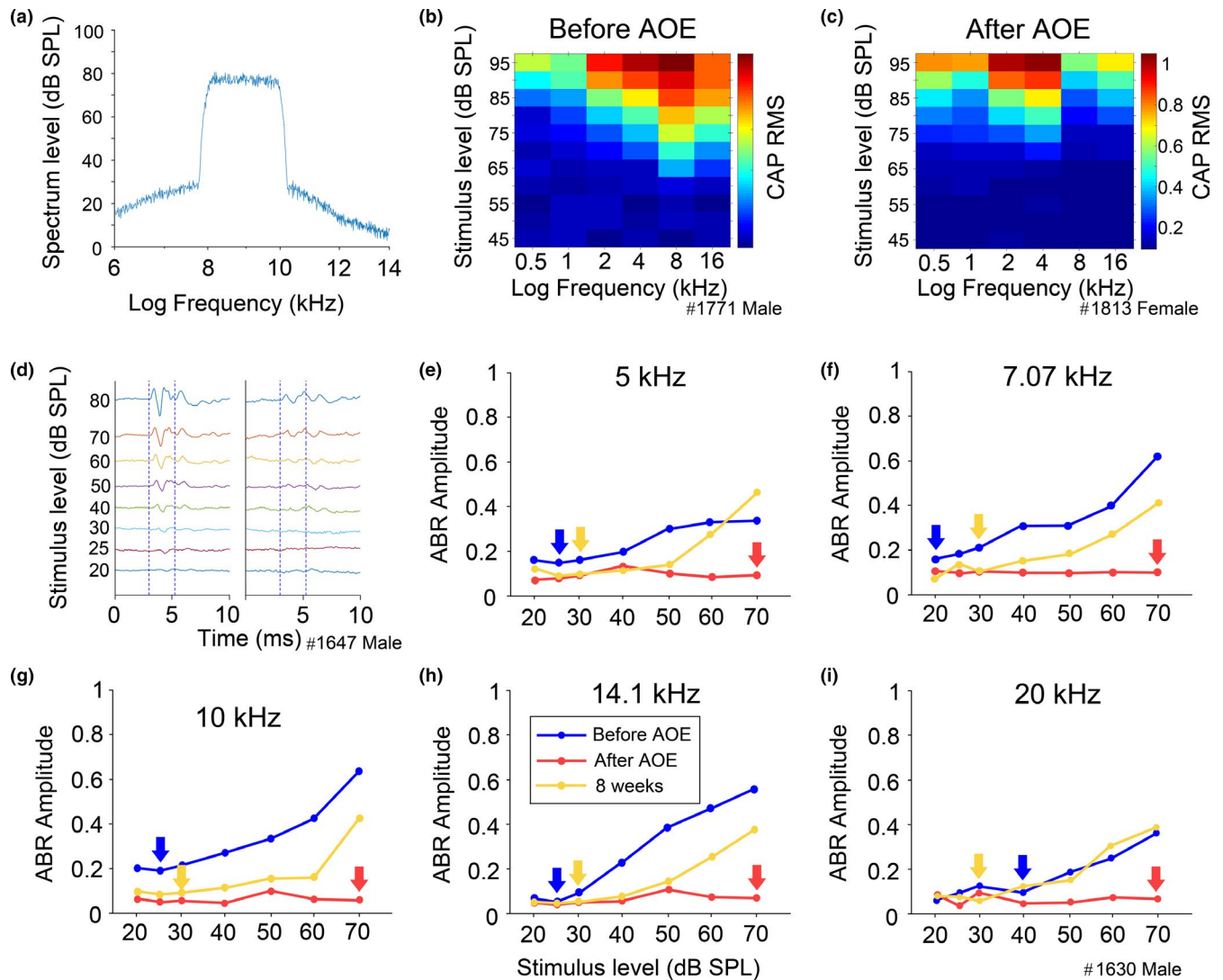


**FIGURE 2** (a) The noise exposure stimulus, as measured close to the ear canal, showing the sharp filter edges at 8 and 10 kHz. (b, c) Compound action potential (CAP) recordings from the round window of a healthy control and one that had been subject to acoustic over-exposure (AOE) 8 weeks previously. The size of the CAP is represented by the colour scale, which shows the root mean square (RMS) value normalised to the highest value for that animal. Thresholds for frequencies up to 4 kHz are unaffected by the AOE, but there is a large elevation in threshold at 8 kHz. (d) Auditory brainstem responses (ABRs) were routinely recorded before and after AOE with a variety of stimulus frequencies and sound levels (10 kHz in this case) and measured in the interval from 3 to 6 ms as indicated by the dotted lines. (e–i) The difference between the highest peak and trough in the measurement window was plotted for each stimulus frequency and sound level and the threshold (marked by an arrow) estimated for each curve. The three curves show the values before, immediately after and 8 weeks after AOE for each stimulus frequency between 5 and 20 kHz

as indicated by arrows in Figure 2e–i. All of the noise-exposed animals showed an initial large increase in threshold, but in some animals, there was a partial recovery of threshold. However, even in these animals, there was still a consistent elevation of threshold after 10 weeks and so every animal showed permanent evidence of hearing loss over the range of 5–20 kHz. In the two animals where the CAP (Johnstone, Alder, Johnstone, Robertson, & Yates, 1979) was measured, we presented tones at a greater range of frequencies starting at 0.5 kHz. The CAP recordings indicated that there was no evidence of any damage in the parts of the cochlea coding frequencies of up to 4 kHz (Figure 2b,c).

Subsequent behavioural analysis allowed us to divide the noise-exposed animals into two groups of 12 tinnitus animals and 14 non-tinnitus animals. We wanted to make sure that hearing loss would not be a factor in altering the results of the behavioural tests and needed to determine whether there was any systematic difference between the hearing levels of the two groups. The pure tone thresholds were measured blind for all the animals before identifying to which group they belonged. The difference between the thresholds before, immediately after and ~10 weeks after AOE was measured in each animal, and then, the means for each frequency were compared in a paired $t$ test. There was no significant difference between the two behavioural groups ($p = .46$). The mean difference between the thresholds before and immediately after AOE for the tinnitus group ($n = 77$) was 27.6 dB ($\pm 6.1$ at one standard deviation) and by 10 weeks was 28.6 dB ($\pm 6.6$). The mean difference between the thresholds before and immediately after AOE for the non-tinnitus group ($n = 79$) was 27.4 dB ($\pm 6.5$) and by 10 weeks was 28.6 dB ($\pm 6.7$). Thus, we were confident that hearing loss by itself did not contribute to the behavioural differences between the two groups.

## 3.2 | Behavioural identification of tinnitus

The behavioural equipment used for detecting GPIAS allowed us to measure the whole-body startle and the pinna displacement simultaneously. However, the ear flick data were much less variable and had a better signal-to-noise ratio than the whole-body startle. An example of this is shown in Figure 3 where the typical pinna movements during no-gap (Figure 3a) and gap (Figure 3b) trials can be compared with the whole-body movements for the same trials (Figure 3d,e). In this instance, the mean pinna amplitude of the gap trials was 29% less than that of the no-gap trials (Figure 3c). We have shown previously (Berger et al., 2013) that the mean signal-to-noise ratio ($\pm SEM$) of the pinna reflex (29.2 $\pm$ 6.2 dB) was substantially higher than that of the whole-body startle (21.4 $\pm$ 3.8 dB). When the coefficient of variance was calculated for the two responses, the pinna reflex responses had ~50% less variability than the whole-body responses. Thus,

only the pinna reflex values were used to calculate GPIAS values. For most animals (19/26), the distribution of pinna deflections observed was normally distributed when tested with a Lilliefors test and an example of the distribution of no-gap responses for one animal is shown in Figure 3g. The mean and median are almost identical. When the no-gap data are summed across all 26 animals, the distribution is bimodal (Figure 3h) because of differences between males and females. The mean deflection for the females was 7.4 $\pm$ 2.45, while the mean deflection for the males was 9 $\pm$ 3.98. When the distribution of mean pinna deflections for all 26 animals was compared with the distribution of the medians, they were found to be very similar (Figure 3i), and this justified the use of a parametric test in the analysis of the data. We did not have to take the log values of the deflections in the way that is necessary for the whole-body data that have a very skewed distribution with large differences between the mean and median (Schilling et al., 2017). The baseline behavioural data were compared with the 7–9 weeks' data using a 2-way ANOVA with Bonferroni's multiple comparison test. If a significant increase in the gap/no-gap ratio was seen at any frequency, the guinea pig was deemed to have tinnitus at this frequency. Tinnitus was observed in 12 animals, at a range of frequencies, either 12–14 kHz ($n = 5$), 16–18 kHz ($n = 5$), 8–10 kHz ($n = 4$), 4–6 kHz ($n = 2$) or broadband noise (BBN; $n = 3$). Evidence of tinnitus was observed at between one and three frequency bands in the tinnitus animals. Figure 3f demonstrates the behavioural data for an animal that showed tinnitus behaviour at 8–10, 12–14 and 16–18 kHz. Details of the 12 animals with tinnitus and the frequency bands where evidence of tinnitus was observed are provided in Table S1.

## 3.3 | The effect of noise exposure and tinnitus on the firing rate of units in the VCN

Recordings were made from 26 noise-exposed animals (11 male and 15 female), of which 12 had developed behavioural evidence of tinnitus (seven male and five female; see Figure S1). The different proportions of males and females developing tinnitus were not significant (Fisher's exact test, $p = .23$). There were a total of 79 single units from non-tinnitus animals and 77 from tinnitus animals. We were able to compare these with recordings from the VCN of 30 control guinea pigs (17 male and 13 female), yielding 131-hr-long recordings (Hockley et al., 2020). The effect of noise exposure on firing rates in the VCN was then analysed. Only well-isolated single unit recordings were used for this analysis. An example of one such unit being stimulated with a 200-ms tone pip at 6 kHz is shown in Figure 4a. The stability of the spike waveform was assessed by superimposing each spike as it was collected (Figure 4b), and by plotting the PSTH of the spike distribution, we were able to confirm that it was an example
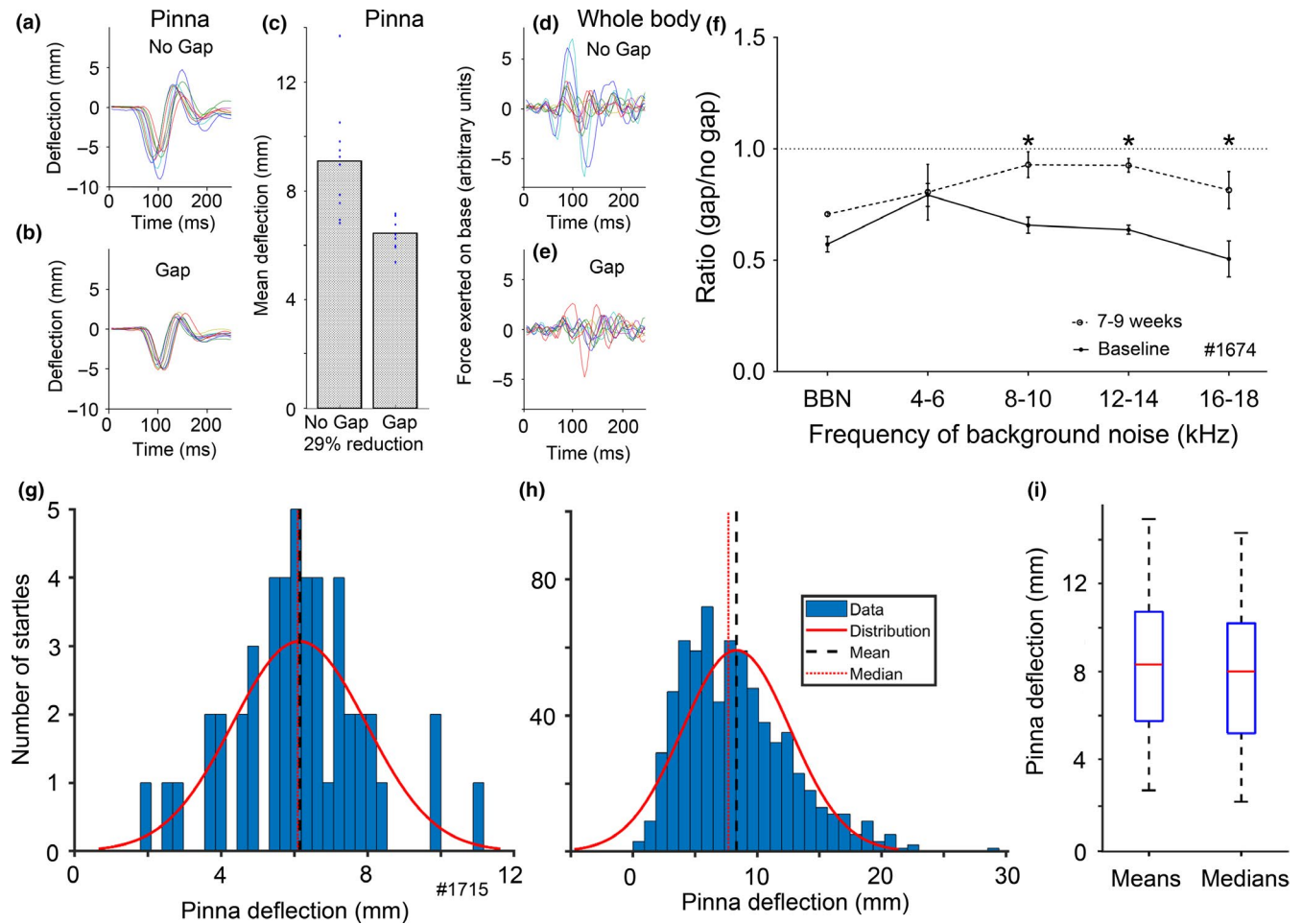
**FIGURE 3** Use of the pinna reflex to provide behavioural confirmation of tinnitus. (a, b) Examples of raw data representing the change in the distance between the pinna in response to a startle pulse with or without a gap in the preceding background broadband noise. (c) The mean deflection for the gap responses is 29% smaller than that for the no-gap background, and for each condition, the response variability is reasonably small. (d, e) By comparison, the amplitude of the whole-body response is much more variable and the signal-to-noise ratio is generally smaller for both the gap and no-gap conditions. (f) The mean ± *SEM* ratio of gap/no-gap startle amplitudes is plotted for each background noise frequency and at different time points (baseline vs. 7–9 weeks postnoise exposure). Asterisks indicate significance at $p < .05$ ($n = 5$ trials). A ratio of 1 represents no difference between the gap/no-gap conditions and 0 indicates full inhibition of the startle by the gap. (g) The distribution of pinna deflections for the no-gap trials in the baseline condition with broadband noise (BBN) background for a representative animal is shown with a normal distribution (red line) superimposed. The mean (black dashed line) and median (red dotted line) are almost identical. (h) The distribution of pinna deflections across all animals is shown with a normal distribution superimposed. In this case, there is a bimodal distribution and the means and medians are slightly different because the means for the male and female animals in the group are different. (i) The distribution of means and medians for all 26 animals are shown as box and whisker plots. Overall, the data are slightly skewed with the medians showing slightly smaller values in seven guinea pigs

of a primary-like neuron (Figure 4c). Confirmation that a single unit had been isolated was also provided online by plotting peak versus trough amplitudes (Figure 4e), and the CF was confirmed offline by plotting a frequency response area (Figure 4d). Each time a new electrode assembly was used, its functionality was tested by the iontophoretic application of glutamate from one of the channels. Most neurons gave a strong response to glutamate, but the response latency varied between about 5 and 30 s. Examples of this variable response latency are shown by the traces in Figure 4f,g. The effect of iontophoretic current being passed by a buffered salt solution was also tested on 15 units using solutions of D-NAME (the

inactive enantiomer of L-NAME; Hockley et al., 2020) and on 8 units with acetate buffer at the same pH and molarity as the SIN-1 solution. Neither the D-NAME nor the acetate buffer had any consistent effect on the recorded activity. An example of the lack of effect of acetate buffer on one neuron is shown in Figure 4h where the spike width (black line) and the spike amplitude (blue line) are both unaffected by the 10-min ejection period. The buffer solutions did not have any consistent effect on the spontaneous firing rate either (Figure 4i).

The first predictions that were tested were those suggesting that both the spontaneous and driven firing rates would
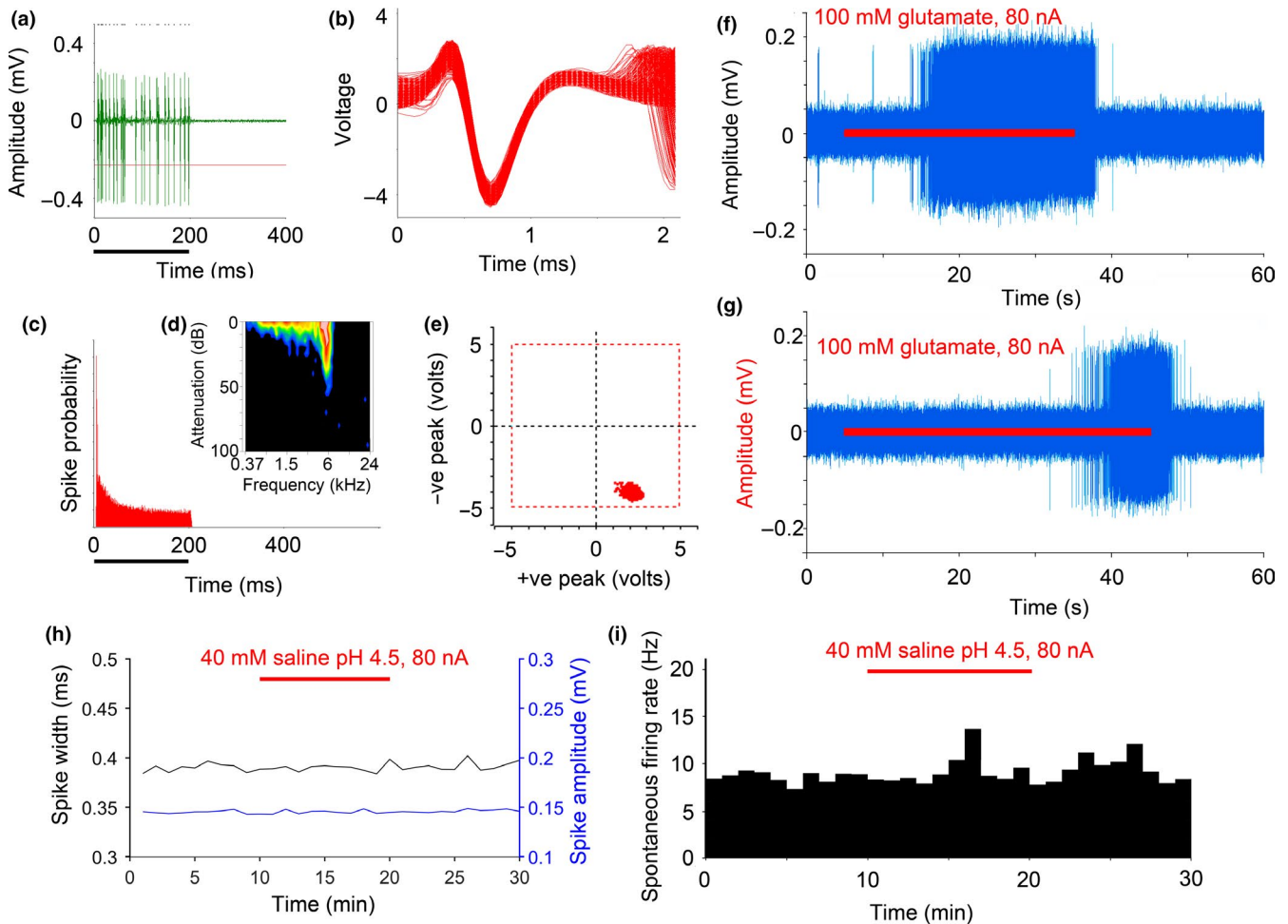
**FIGURE 4** (a) Example of online analysis of a single unit (CF, 6 kHz) stimulated with a 200-ms tone (black bar under trace) at 70 dB SPL viewed in the Brainware programme showing the spike timings (black raster), spike shapes (green) and detection threshold (red line) over a single sweep. (b) The superimposed spike waveforms confirm that the spike waveform remained constant. (c) A rolling average PSTH across sweeps. This unit displayed a primary-like PSTH. (d) The characteristic frequency of the unit was measured using a frequency response area analysis, and this was plotted offline later. (e) Spike stability was also assessed by plotting positive versus negative peak amplitude during the recording. (f) When the first unit of a new track was isolated, 100 mM glutamate was applied (horizontal red bar) to check the responsiveness of the unit. Most units responded very strongly to glutamate, and for this unit, there was a rapid increase in firing rate within 10 s. (g) Single unit with a slower and more gradual response to glutamate where the response delay was over 25 s. (h) Five units were tested with a control, buffered saline solution where SIN-1 was replaced by acetate buffer in a solution of sodium chloride at the same pH and molarity. There was no significant effect on the spike width (black line) or amplitude (blue line) when applying this solution for 10 min (horizontal red bar) as shown in this example. (i) Applying the buffered saline solution had no significant effect on the spontaneous firing rate either, as shown by this unit

be similar or greater in the tinnitus animals than in the control ones and that both these groups would have higher firing rates than the non-tinnitus group. Figure 5 shows the spontaneous and driven firing rates measured from the three groups of animals. Neurons from non-tinnitus animals had a significantly lower driven firing rate ($144 \pm 87$ sp/s; $n = 77$; median $= 119$ sp/s) than tinnitus animals ($175 \pm 116$ sp/s; $n = 76$; median $= 141$ sp/s). As the data strongly deviated from having normal distributions, they were analysed with a Kruskal–Wallis test with Dunn's multiple comparison test, $p = .0343$. The significant difference between the tinnitus and non-tinnitus animals was due more to reduced firing rates in

the non-tinnitus animals (compared with controls where the mean was $148 \pm 98$; $n = 130$; median $= 136$ sp/s) rather than higher firing rates in the tinnitus animals. Significantly higher mean spontaneous rates were observed in the VCN of tinnitus animals ($40 \pm 44$ sp/s; median $= 28$ sp/s) compared with controls ($27 \pm 32$ sp/s; median $= 15$ sp/s; Kruskal–Wallis test with Dunn's multiple comparison test, $p = .0119$), and compared with rates from non-tinnitus animals ($26 \pm 28$ sp/s; median $= 14$ sp/s; Kruskal–Wallis test with Dunn's multiple comparison test, $p = .0490$). When these data were divided by cell type, no cell-type-specific changes in spontaneous firing rate were found. The group that came closest to reaching
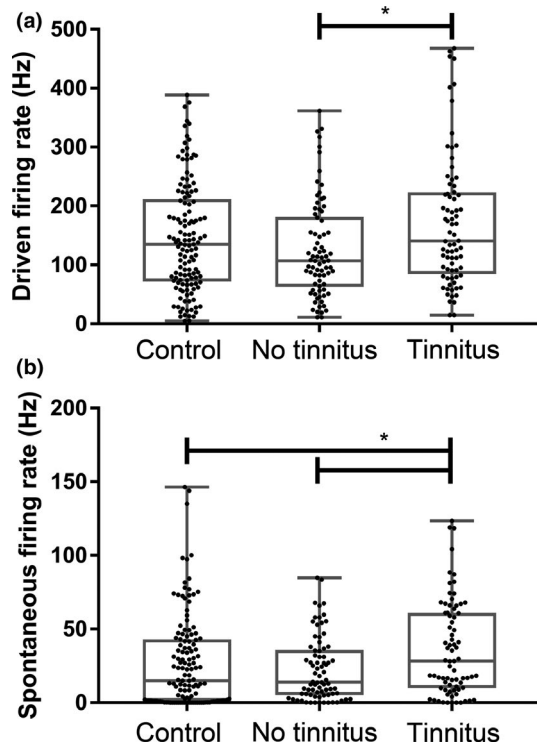
**FIGURE 5** Box and whisker plots displaying median, quartiles and ranges of driven and spontaneous firing rates of VCN units from control (n = 130) and experimental animals. Units from noise-exposed animals with behavioural evidence of tinnitus (n = 76) exhibit higher driven firing rates to tones at 20 dB above CF threshold than those from noise-exposed animals without behavioural evidence of tinnitus (n = 77). Tinnitus animals also show increased spontaneous rates compared with control or no tinnitus animals

significance for a change in spontaneous firing rate was the chopper cells of which there were 21 in the tinnitus group (T, mean rate = 35.4 sp/s), 19 in the non-tinnitus group (NT, mean rate = 30.8 sp/s) and 53 in the control group (C, mean rate = 23.2 sp/s). These were compared with a Kruskal–Wallis

test ($p = .12$). There were slightly smaller numbers of cells in the primary-like group (T, 16 cells, mean rate 35.6 sp/s; NT, 16 cells, mean rate 29.4 sp/s; and C, 23 cells, mean rate 47.9 sp/s) and $p = .22$ in the Kruskal–Wallis test. There were even smaller numbers in the onset group (T, five cells, mean rate 7.9 sp/s; NT, six cells, mean rate 7 sp/s; and C, 18 cells, mean rate 12.7 sp/s) and $p = .62$ in the Kruskal–Wallis test. Although spontaneous rates were reduced in non-tinnitus animals compared with controls, this change did not reach significance when all the cell types were combined. There were not enough units recorded in any of the groups to determine whether the changes were associated with a particular frequency band. Thus, following noise exposure, both the spontaneous and driven firing rates are reduced in the non-tinnitus animals, while in the tinnitus animals, the driven firing rate remains the same as in controls, but there is an increase in the spontaneous firing rate. These results seem to confirm predictions 1 and 2.

## 3.4 | Iontophoresis of NO donor in noise-exposed animals

The next prediction we tested was that the units in the tinnitus animals would have an altered sensitivity to an NO donor compared with the control or non-tinnitus groups. The NO donor SIN-1 was applied to 25 units from four control animals, 24 from three non-tinnitus animals and 25 from four tinnitus animals. We measured three relevant parameters where there could be either an increase or a decrease. These were driven firing rate, spontaneous firing rate and spike width as described previously (Hockley et al., 2020). These measurements allowed us to confirm that, as predicted, the number of units showing an effect on at least one of these parameters in the T group (14/25; 56%) was greater than in the control group (6/25; 24%). However, contrary to our predictions, the

**FIGURE 6** (a) PSTH of a chopper unit (CF 3 kHz) from a tinnitus animal over the initial 5 min (sweeps 1–300). Inset figure shows the chopping pattern of this unit. (b) The PSTH of the same neuron following 120 nA SIN-1 application, resulting in increased driven rate and reduced spontaneous rate (sweeps 2,701–3,000). The inset shows the steady waveform of the individual spikes. (c) The change in PSTH during 120 nA SIN-1 application. An increase in driven firing rate and a decrease in spontaneous firing rate are observed. Bin size = 0.5 ms. A two-sample Kolmogorov–Smirnov test confirmed the distributions are significantly different ($p < .01$). (d) The mean ($\pm$ SD) spike rate for a VCN chopper unit (CF 3 kHz) from a tinnitus animal during each analysis period. Significant increases and decreases were observed in driven (solid line) and spontaneous (dashed line) firing rates, respectively, during SIN-1 application. (e) Example of a spike waveform from a chopper unit of a tinnitus animal taken as the mean of 5 min during baseline and the last 5 min of SIN-1 application at 120 nA. There was a large increase in both the amplitude and the width (85%) of the waveform (red line). (f) Example of a spike waveform from a non-tinnitus animal with an unclassified unit (CF 12 kHz), where there was a decrease in the amplitude (29%, red line) after the application of SIN-1 (120 nA), but no change in the spike width at half amplitude. (g) Spike-rate histogram of an unclassified unit (CF 1 kHz) from a non-tinnitus animal (bin size = 10 s) over 1 hr. Three periods of SIN-1 ejection at varying strength are indicated by the horizontal red lines, and there is a corresponding increase in the spontaneous firing rate. (h) Spike-rate histogram from the same chopper unit as in (a) showing the decrease in spontaneous firing rate over an hour in response to the three periods of SIN-1 ejection. (i) Spike-rate histogram of an unclassified unit (CF 12 kHz) from a non-tinnitus animal showing a prominent increase in the driven firing rate in response to three periods of SIN-1 ejected over 1 hr. (j) Spike-rate histogram of chopper unit (CF 4 kHz) from a non-tinnitus animal showing a cumulative decrease in the driven firing rate in response to three periods of SIN-1 ejected over 1 hr
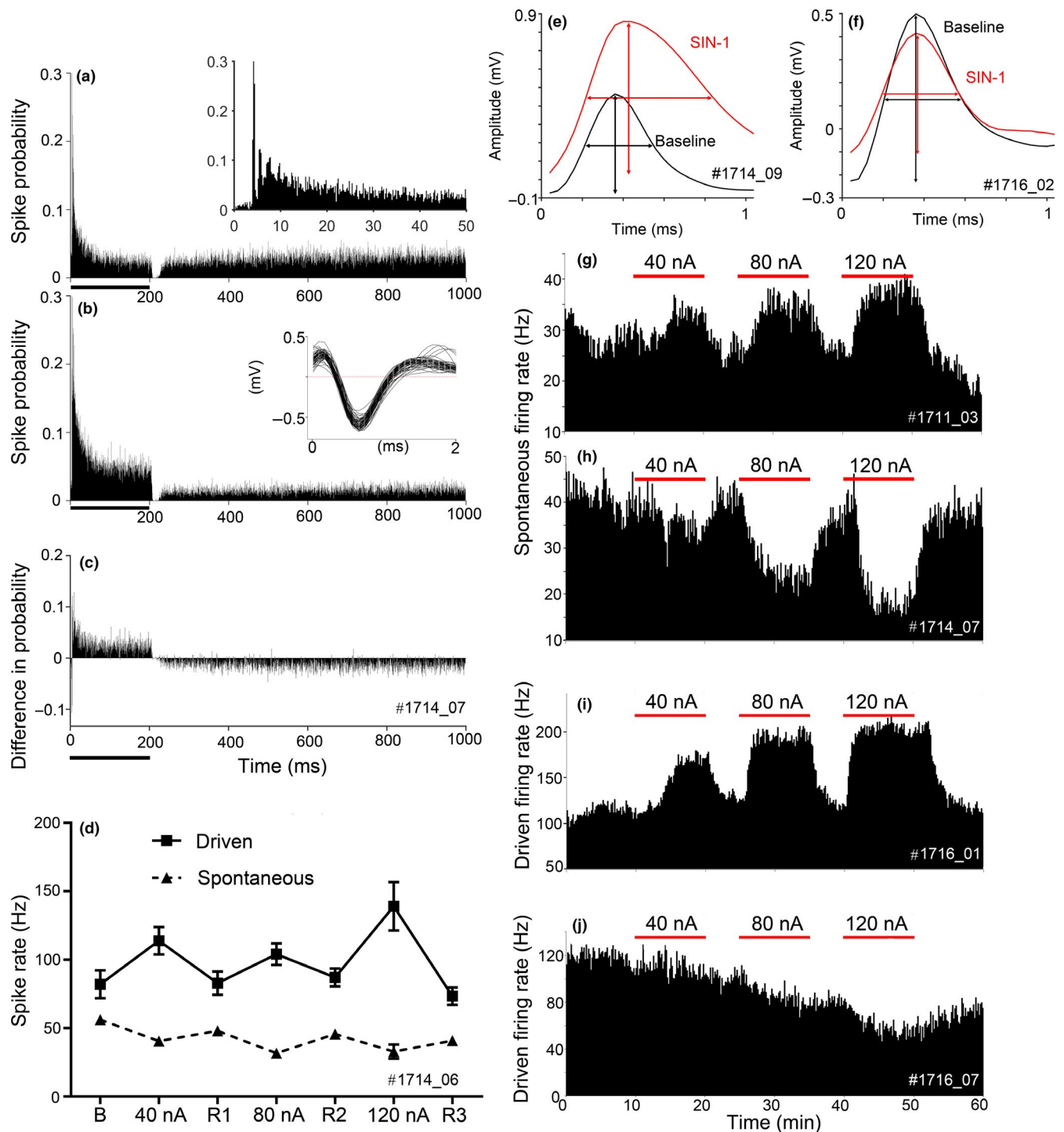
group with the highest number of responsive cells was the non-tinnitus group (17/24; 71%).

Following SIN-1 application, five of 25 units in control animals showed increases in the driven activity, with a decrease observed in the spontaneous activity in one unit. Two of the units with increased firing rates also showed increases in spike width. Following noise exposure, a greater range of effects was seen, with some units from both the tinnitus and non-tinnitus groups showing either increases or decreases in spontaneous and/or driven firing rate. Both groups also

showed examples of increased spike width, although only the non-tinnitus group contained units with decreased spike width ($N = 2$). The three parameters could change independently of each other, and across the tinnitus and non-tinnitus groups, 14 units showed a change in one parameter alone, 14 units showed a change in two of the parameters together, and three units showed an increase in all three parameters. Examples of the types of changes seen are shown in Figure 6. One particularly interesting combination of effects was that in two chopper units from a tinnitus animal, there was a simultaneous
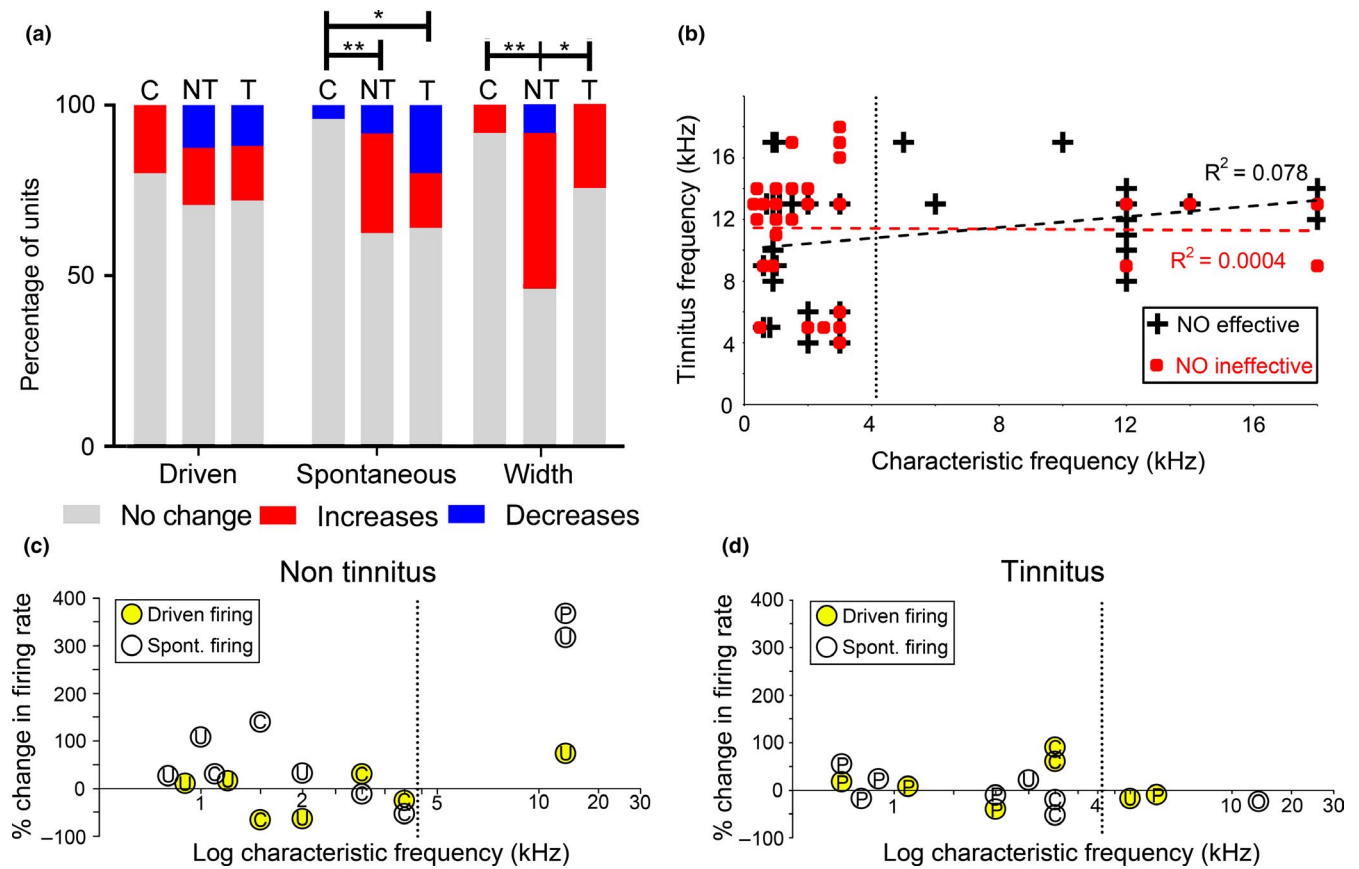
**FIGURE 7** (a) The proportion of VCN units significantly increasing or decreasing their firing rates or spike width during SIN-1 application, for driven and spontaneous periods and each animal class (C, NT and T). (b) Plot showing the relationship between CF of units and the estimated centre frequency of tinnitus in that animal. The black crosses show units where changing the NO levels with SIN-1 or L-NAME produced a change in firing rate and/or spike shape, while the red squares show units where altering NO levels had no effect. The dashed regression lines show there was no systematic relationship between characteristic frequency and tinnitus frequency in either group. The black dotted line in this and the lower panels shows the approximate border between units that did or did not have a significant change in threshold produced by the noise exposure. (c, d) Plots of the percentage change in firing rate produced by applying 120 nA in the SIN-1 electrode for units of different CF in the non-tinnitus and tinnitus groups. The different backgrounds of the markers indicate whether the change was for spontaneous or driven rates. The letters indicate the type of unit: C, chopper; P, primary-like or phase-locking; O, onset; U, undefined

increase in their driven firing rate and decrease in their spontaneous firing rate during SIN-1 application. This effect of a rate-dependent reversal of the NO effect was not observed in any other units from control, non-tinnitus or tinnitus animals with either of the iontophoretically applied drugs. Figure 6a,b shows the PSTHs for one of these units before and during the application of SIN-1 using 120 nA injection current. The difference in PSTH (Figure 6c) clearly shows the increase in driven firing rate occurring at the same time as the reduction in spontaneous firing rate. Figure 6d shows the driven and spontaneous firing rates during seven analysis periods for the other chopper neuron. When the SIN-1 was applied, the driven firing rate increased during the drug application, and fell back to the baseline during the three recovery intervals (R1–R3). Conversely, the spontaneous discharge rate in these two units, measured during the drug application, decreased, but recovered to baseline values in the recovery intervals. Both spike width and amplitude were measured and could

vary independently of each other as shown in Figure 6e,f. In Figure 6e, there was a large increase in the spike width (85%) following application of SIN-1 and the amplitude increased by 53%. However, for the unit shown in Figure 6f, there was a 29% decrease in spike amplitude but no significant change in the spike width following the application of SIN-1. The effects of SIN-1 were concentration-dependent, and clear examples of monotonic increases or decreases in firing rate with increasing levels of electrode current are shown in Figure 6g–j. Units could show either an increase in the spontaneous rate (Figure 6g) or a decrease (Figure 6h). The driven firing rate could also increase (Figure 6i) or decrease in response to the SIN-1 (Figure 6j). The response in the latter unit appeared to be cumulative as the baseline driven firing rate did not fully recover before the next application of SIN-1.

The overall differences in the proportions of units that increase their firing rate or spike width in response to SIN-1 are shown in Figure 7a for control (C), non-tinnitus (NT) and

tinnitus (T) animals. There are clearly differences between the control and noise-exposed groups but, perhaps as a result of the relatively small sample sizes, the differences in driven firing rate do not reach significance. The numbers of units that showed an increase, decrease or no change in the three experimental groups were placed in a $3 \times 3$ grid for each parameter. Fisher's exact tests of each of the $3 \times 3$ tables showed no significant differences for driven activity ($p = .474$), but significant differences in the spontaneous data ($p = .006$) and spike width ($p = .003$). Further, Fisher's exact tests determined this difference was due to significant differences between control and non-tinnitus ($p = .004$) and control and tinnitus ($p = .013$) groups, with no significant difference between tinnitus and non-tinnitus ($p = .384$) groups for the spontaneous firing rates. For the spike width, there were significant differences between the non-tinnitus and both the control and tinnitus groups but no significant difference between the control and tinnitus groups. This is summarised graphically in Figure 7a.

It might be expected that it would be the neurons with CFs closest to the tinnitus frequencies, identified in the behavioural work, which would be most likely to show an increase in their sensitivity to NO. However, we found no evidence to support this suggestion. To examine this relationship, we plotted the CF of neurons, which either were or were not sensitive to changes in NO levels, against the identified tinnitus frequency (listed in Table S1). Data were included from cells that were tested with both SIN-1 and L-NAME, and the resulting plot is shown in Figure 7b. There was no significant difference between the two populations. One possible reason for this might be that it was the strength or direction of the effect induced by the SIN-1 application that differed between the tinnitus and non-tinnitus populations and not just the presence or absence of an effect. Thus, we next plotted the CF of identified neurons against the change in either spontaneous or driven firing rate in response to SIN-1. This allowed us to divide the neurons into those with high-frequency inputs, where the afferent input should be reduced, and those with low-frequency input where there should be less change in the inputs. The plots are shown for the non-tinnitus animals in Figure 7c and for the tinnitus group in Figure 7d. The main difference between the two plots is that for the three high-frequency neurons (those to the right of the black dotted line) in the non-tinnitus group, there is an increase in firing rate, whereas for the tinnitus group, the three high-frequency neurons all show a decrease in firing rate. This is further evidence that NO function is different in the tinnitus and non-tinnitus animals, although the small number of units makes it difficult to assess the significance.

Another possible source of difference between the tinnitus and non-tinnitus animals would be in the types of neurons that were sensitive to exogenous NO. The different letters superimposed on the symbols in Figure 7c,d show the variety

**TABLE 1** Number of cell types changing firing rate in response to SIN-1

| Type | Control | Non-tinnitus | Tinnitus |
|---|---|---|---|
| Primary | 2 | 1 | 8 |
| Chopper | 4 | 6 | 2 |
| Undefined | 1 | 4 | 2 |

of cell types recorded in each of the experimental groups. Most of the cells with phase-locking responses appeared to be primary-like and so these two groups were combined. Only one onset cell in both the control and tinnitus groups was identified and so these were not included in the analysis of differences. This left three main types of neurons, and the numbers of each in the three experimental groups are shown in Table 1. The PSTHs used to classify the units are shown for the tinnitus group in Figure S1. The $3 \times 3$ array was analysed with a Fisher's exact test with Freeman and Halton (1951) extension to assess the probability that the neuron types in each experimental group had the same underlying distributions and they were found to be significantly different ($p = .046$). The main cause for the difference between the groups was the different numbers of primary-like and chopper neurons in the tinnitus and non-tinnitus groups. When a Fisher's exact test was applied to a $2 \times 2$ array with these data, it was significantly different ($p = .015$). This indicates that following noise exposure, a greater proportion of primary-like neurons became sensitive to SIN-1 in the tinnitus group, while in the non-tinnitus group, it was the proportion of chopper neurons that mainly increased.

## 3.5 | Inhibition of NOS by L-NAME in noise-exposed animals

The fourth prediction was that "Blocking endogenous NO production will reduce the driven firing rate of more neurons in the tinnitus group than in the control and non-tinnitus groups." This was based on the assumption that increased levels of endogenous nitric oxide in tinnitus animals would produce a chronic increase in the firing rates of many neurons in the VCN. To test this, we applied a nNOS blocker (L-NAME) while recording from single units in the tinnitus and non-tinnitus groups and compared the effects to the units recorded previously in the control group. Measurements were made from single units in nine control (22 units), five non-tinnitus (22 units) and four tinnitus (19 units) animals. The driven firing rate during the final 10 min of drug ejection was compared with both the final 10 min of baseline and the final 10 min of the recovery period using a Kruskal–Wallis test with Dunn's multiple comparison test. Only changes in firing rate that were significantly different from the baseline rates before and after drug ejection were accepted as real.
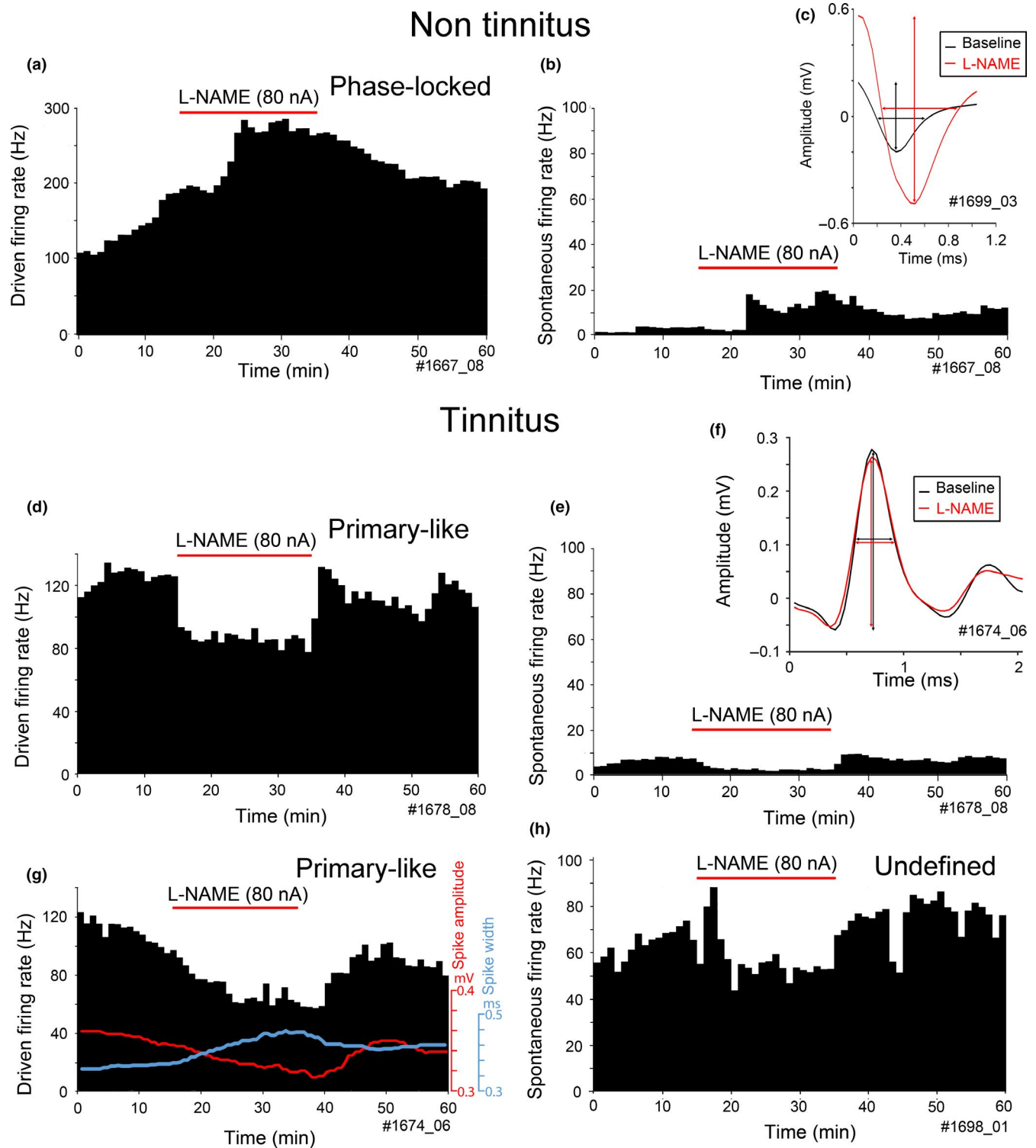
Application of L-NAME to control animals could produce an increase in driven firing rate or spontaneous firing rate or sometimes both, and this was also true in the non-tinnitus animals. An example from a non-tinnitus animal is shown in Figure 8 where there was an increase in both the driven firing rate (Figure 8a) and the spontaneous rate (Figure 8b) in the same unit. In this unit, there was a delay of over 5 min before any effect was seen. Some other units had a faster response, but the effect usually took minutes to develop rather than seconds. In the non-tinnitus animals, the change in firing rate, if present (10/22), took between 2.5 and 17 min to start (mean $8.6 \pm 4.2$ min). The start of the response was taken as the first of three consecutive bins where there was a change of more than 10% from the baseline firing rate. In the control animals, the application of L-NAME never produced a decrease in driven activity, and in the non-tinnitus animals, there was only one neuron (1/22, 4.5%) where L-NAME produced a decrease in driven activity (unclassified, CF 18 kHz). By contrast, there were seven neurons from the tinnitus group (7/19, 37%) where there was a decrease in the driven activity in the presence of L-NAME. An example of one of these cells is shown in Figure 8d where there is a rapid fall in firing rate when the current is turned on and then a rapid increase when the current is turned off. In this unit, there was also a significant change in the spontaneous firing rate during L-NAME application, and this was also true of five of the seven tinnitus neurons with a decrease in driven firing rate where there was also a decrease in the spontaneous rate. In most of the neurons from tinnitus animals, the effect of the L-NAME on firing rate was more gradual and an example of this is shown for another primary-like neuron in Figure 8g. There was a gradual reduction in driven firing rate over a period of about 10 min, and then, the firing rate remained relatively stable before starting to increase again about 5 min after the L-NAME current was switched off. This unit did not show any significant change in spontaneous firing rate, but an example of decreased firing rate in a neuron (undefined, CF 5 kHz) where there was more of a delay before the change started (3.5 min) is shown in Figure 8h. The delay in the start

of the change in firing rate for 11 neurons from tinnitus animals ranged between 0.5 and 10.5 min (mean $4 \pm 3.4$ min). This was significantly faster than in the non-tinnitus group ($t$ test, $p = .006$).

One way in which nitric oxide might be changing neuronal excitability is by altering the properties of membrane channels. A change of this sort could give rise to alterations in the shape of the action potential. Thus, we measured the spike width at half amplitude before and during the L-NAME application. An example of the changes seen is shown in Figure 8c where there is a large (52%) increase in the spike width after L-NAME application. In this example, there was also an increase in spike amplitude but that was not always the case as there could be an increase in spike width along with a decrease in spike amplitude as shown in Figure 8f. The changes in spike width were usually quite gradual as illustrated in Figure 8g where the spike width (blue line) and spike amplitude (red line) are plotted over the duration of the experiment. The mean spike width over the last 5 min of the L-NAME application had increased by 21%. In the tinnitus animals, five neurons (5/19, 26%) showed a significant change in spike width during L-NAME application of 2%–21%. The non-tinnitus animals had the same number of units where there was a significant change in spike width (5/22, 23%), and the changes varied from 2% to 35%. The two groups showing changes in spike width were too small to assess the significance of the differences between tinnitus and non-tinnitus animals.

In the populations as a whole, L-NAME application to VCN units from control animals resulted in increases in the driven firing rate in a small number of units (4/22, 18%); no decreases in firing rate were observed (Figure 9a). The driven firing rates for the non-tinnitus animals showed similar effects of L-NAME with three neurons (3/22, 14%) showing an increase and one neuron showing a decrease (Figure 9c). However, the effects of L-NAME on the driven firing rate in the tinnitus population were very different (Figure 9e). There were seven neurons showing a decrease (7/19, 37%) and only two showing an increase (2/19, 10.5%). By contrast,

**FIGURE 8** Spike-rate histograms of firing rates (bin size = 10 s), recorded from single units over 1 hr, showing the effect of a single period of L-NAME ejection at 80 nA indicated by the horizontal red line. (a) Driven firing rate of a phase-locked unit (CF 0.9 kHz) from a non-tinnitus animal where there is an increase in the firing rate, corresponding to the L-NAME ejection, after a delay of about 7 min. (b) Spontaneous firing rate, in the same unit, showing a delayed increase about 7 min after the start of the L-NAME ejection. (c) Mean waveform of a primary-like unit (CF, 7 kHz) collected over 1 min during the baseline compared with the mean waveform of the same unit from 1 min towards the end of the L-NAME application. The spike width at half amplitude had increased by 52%. (d) Driven firing rate of a primary-like unit (CF 0.6 kHz) from a tinnitus animal. The L-NAME ejection coincides with a corresponding rapid decrease in the driven firing rate followed by an equally rapid increase when the current is turned off. (e) Spontaneous firing rate in the same unit showing a distinct reduction in the firing rate during the application of L-NAME. (f) Mean waveform of unit shown in (g) collected over the last minute of the baseline compared with the mean waveform of the same unit from the last minute of L-NAME application. The spike showed a slight decrease in amplitude and a 12% increase in width. (g) Driven firing rate of a primary-like unit (CF 1 kHz) from a tinnitus animal. The L-NAME ejection coincides with a more gradual decrease in the firing rate. At the same time, the spike amplitude (red line) gradually decreases and the spike width (blue line) gradually increases. (h) Spontaneous firing rate from an undefined unit (CF 5 kHz) from another tinnitus animal showing a delayed reduction in the firing rate during the application of L-NAME

## Non tinnitus



(a) L-NAME (80 nA)  Phase-locked

(b)

(c) Baseline / L-NAME #1699_03

## Tinnitus

(d) L-NAME (80 nA)  Primary-like

(e)

(f) Baseline / L-NAME #1674_06

(g) Primary-like  L-NAME (80 nA)  Spike amplitude / Spike width #1674_06

(h) L-NAME (80 nA)  Undefined #1698_01

the changes in the spontaneous firing rate in the presence of L-NAME were fairly similar across the three groups (Figure 9b,d,f). The number of neurons showing changes in spontaneous rate were greater in the two noise-exposed groups than controls, but all three groups contained a mixture of neurons with some increasing and others decreasing. The variety of neuronal types and the changes in firing rate for the units that were affected by L-NAME in the tinnitus group are

shown in Figure S2. To study the significance of the changes caused by L-NAME, the results were placed in $3 \times 3$ tables for increases, decreases and constant firing rate for the control, tinnitus and non-tinnitus groups. Fisher's exact tests with a Freeman and Halton (1951) extension on each table showed significant differences in the driven data ($p < .001$), but not spontaneous ($p = .392$). Further Fisher's exact tests between groups of the driven data revealed significant differences
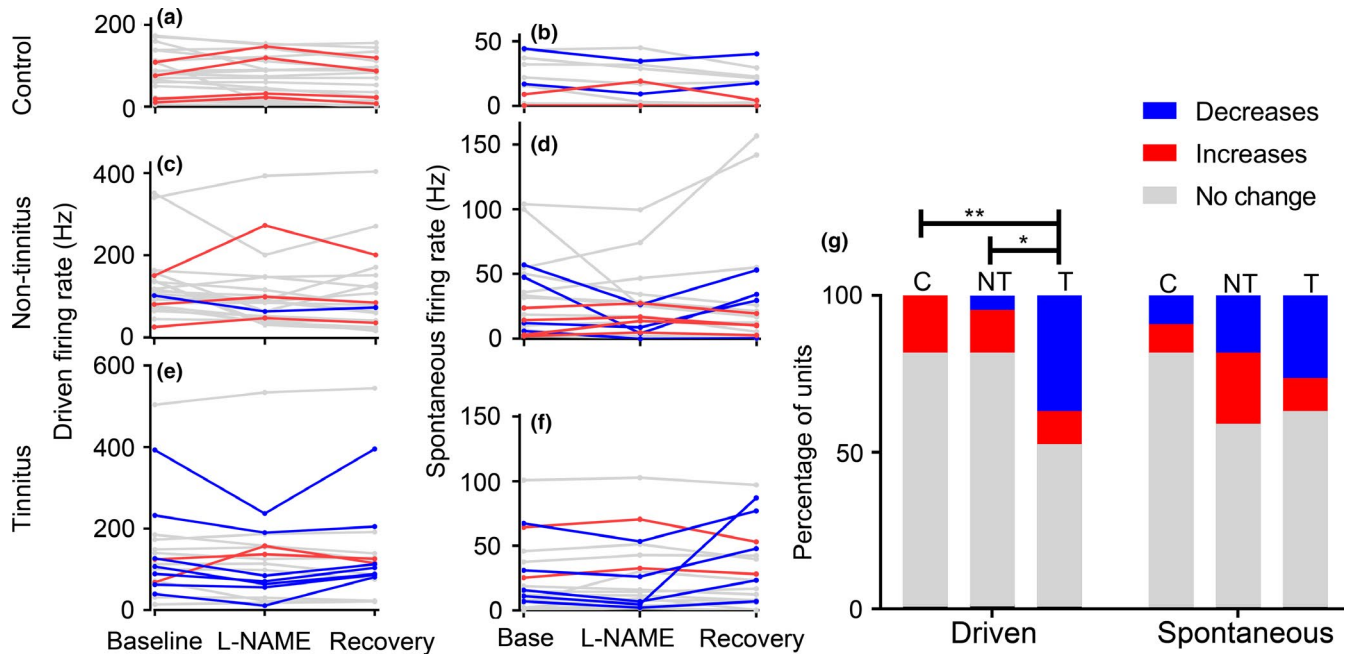
**FIGURE 9** The mean spike rates for each VCN unit during each analysis period. Changes in driven (left) and spontaneous (right) firing rates following L-NAME application, for control (a, b), non-tinnitus (c, d) and tinnitus animals (e, f). Red and blue lines highlight significant increases and decreases, respectively, with grey lines showing all other units. (g) The proportion of units significantly increasing and decreasing their spontaneous and driven firing rates in response to iontophoretic L-NAME application, for control (C), non-tinnitus (NT) and tinnitus (T) animals

between control and tinnitus ($p = .004$) and non-tinnitus and tinnitus ($p = .041$), but not control and non-tinnitus. This is illustrated graphically in Figure 9g. These reductions in driven firing rate, during inhibition of NOS, suggest endogenous NO is chronically increasing the excitability of relay neurons in tinnitus animals.

## 3.6 | Inhibition of NOS during NMDA-evoked excitation in noise-exposed animals

Finally, we predicted that if NMDA channels are involved in the increased driven firing rates of tinnitus animals due to increased NO production, then blocking endogenous NO production should reduce the effect of NMDA application. The effect of L-NAME on NMDA-mediated excitation was characterised in seven control animals, five non-tinnitus and four tinnitus animals. In control animals, NMDA evoked an increase in neuronal firing rate in 15 of 32 (47%) of units with no correlation to cell type or initial firing rate. Similarly, in both non-tinnitus and tinnitus animals, the proportion of units where NMDA increased the firing rate was 17/33 (52%). In the control animals, 40% (6/15) of the NMDA-sensitive units showed an enhanced firing rate in the presence of L-NAME and none showed a reduction in firing rate. Slightly higher proportions were shown by the non-tinnitus group where 59% (10/17) of the NMDA-sensitive units showed an enhanced firing rate in the presence of L-NAME and 12% (2/17)

showed a reduction in firing rate. In marked contrast, the main effect of L-NAME observed in the tinnitus group was a reduction in the response to NMDA. Thus, in the tinnitus group, 35% (6/17) of units showed a reduced firing rate to the bursts of NMDA when it was combined with L-NAME. Only 6% (1/17) of units in the tinnitus group showed an enhanced firing rate when the L-NAME and NMDA were combined.

The effects of L-NAME in enhancing NMDA-induced increases in firing rate were observed in all the main classes of neuron in the non-tinnitus group, and examples are shown in Figure 10a,b for an onset and chopper cell. The one-minute-long bursts of NMDA are indicated by the short green lines, and initially, there was a build-up effect where the initial one or two bursts had little, if any, effect on the firing rate, but then, the effect became cumulative and increased up until the fourth or fifth burst of the series. In these two units, the presence of continuous L-NAME ejection (long red line) facilitated the effect of the NMDA and led to a much stronger effect on the firing rate. Ten minutes after the L-NAME current had been switched off, the effect had largely worn off and the firing rate in response to NMDA alone had returned to levels that were similar to those at the start. In the tinnitus group, the opposite effect was more often seen where the presence of the L-NAME suppressed the increased firing rate produced by the NMDA. Examples of this type of response from an unclassified and chopper neuron are shown in Figure 10c,d. For these two units, there was a cumulative increase in the firing rate for the first four or five bursts of
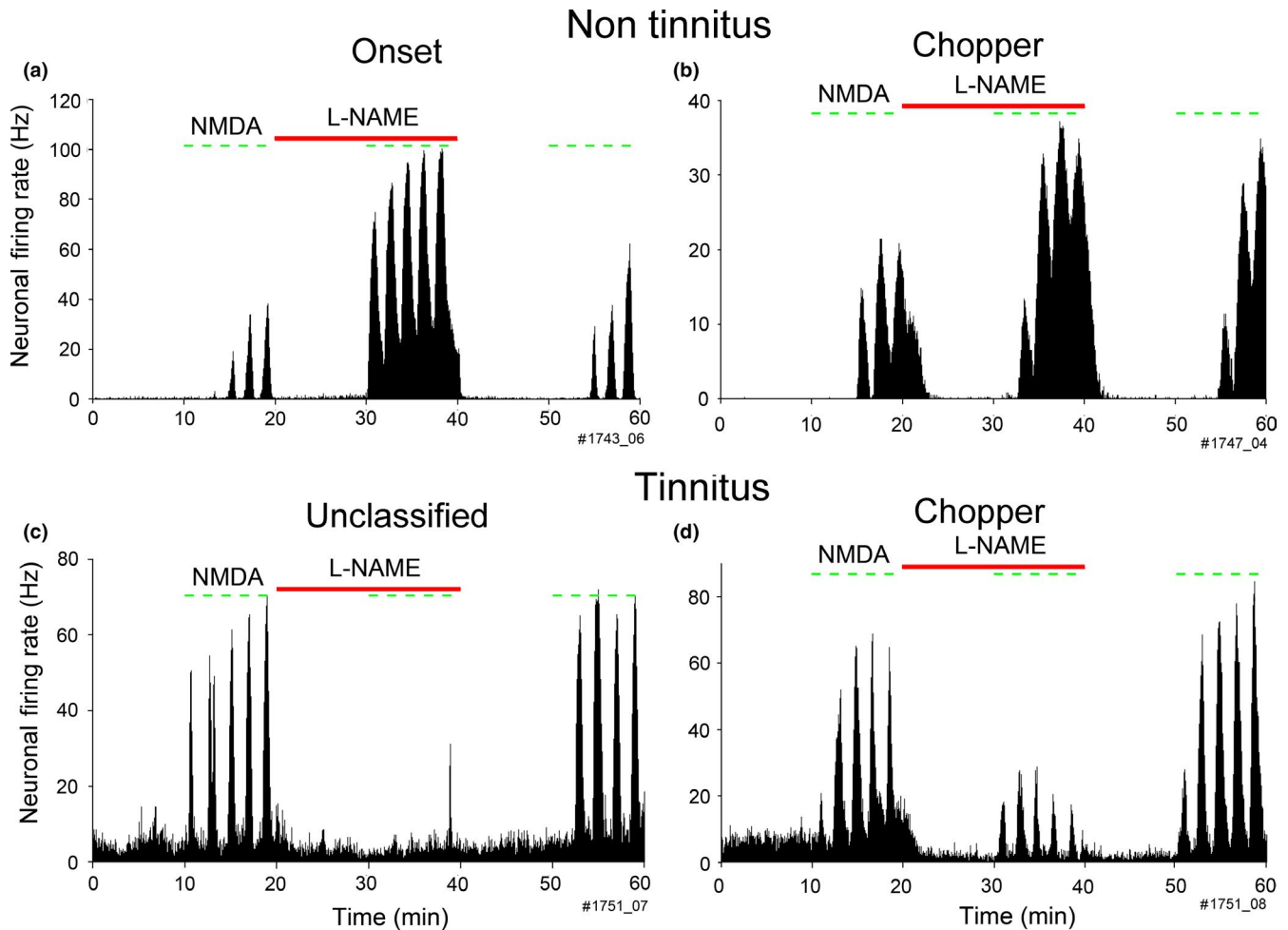
**FIGURE 10** (a, b) Responses of units from noise-exposed animals with no behavioural evidence of tinnitus. (a) Spike-rate histogram of an onset cell, which shows an increase in non-driven firing rate during 1-min bursts of NMDA application (short green bars). Bin size = 10 s. Enhancement of this NMDA-evoked excitation occurred during the 20-min L-NAME application (long red bar). (b) Spike-rate histogram of a chopper cell that also shows an increase in firing rate during NMDA application that is enhanced during L-NAME application. (c, d) Responses of units from noise-exposed animals with behavioural evidence of tinnitus. (c) Spike-rate histogram of an unclassified unit showing that the application of L-NAME greatly reduces the responses to 1-min periods of NMDA application. (d) Spike-rate histogram of a chopper unit showing that the application of L-NAME greatly reduces the responses to 1-min periods of NMDA application

NMDA, but when the L-NAME was applied, the responses became much smaller. Again, after a 10-min recovery period, the NMDA responses recovered to a similar level as that seen before L-NAME was applied.

The significance of the changes in the effects of L-NAME on the NMDA responses in the sampled units from the three groups was assessed by using a Fisher exact probability test with a Freeman and Halton (1951) extension to compare the 3 × 3 grid. This was formed by the units in the control, non-tinnitus and tinnitus groups, and the categories of increased, decreased or unchanged. To determine whether the L-NAME produced a significant increase or decrease in the NMDA-induced firing rate, a Kruskal–Wallis test with Dunn's multiple comparison test was applied to each unit as described in the last paragraph of Methods section. It was highly unlikely that the sampled units from the three groups

could have been taken from populations with the same properties ($p = .0019$). When 2 × 2 grids were used to compare the different groups directly using the increased/decreased categories, then there were highly significant differences between the control and tinnitus groups ($p = .0047$) and between the non-tinnitus and tinnitus groups ($p = .0063$), while there was no significant difference between the control and non-tinnitus groups ($p = .529$).

The recordings confirmed that all the main types of neuron in the VCN could respond to NMDA and have their firing rate modified by L-NAME application. Among the non-tinnitus group, all the main types gave examples where L-NAME increased the response to NMDA and it was only a few chopper cells that showed a decrease (Figure 11a). In the tinnitus group, the situation was different with neurons showing unclassified, phase-locked or chopper responses all showing a
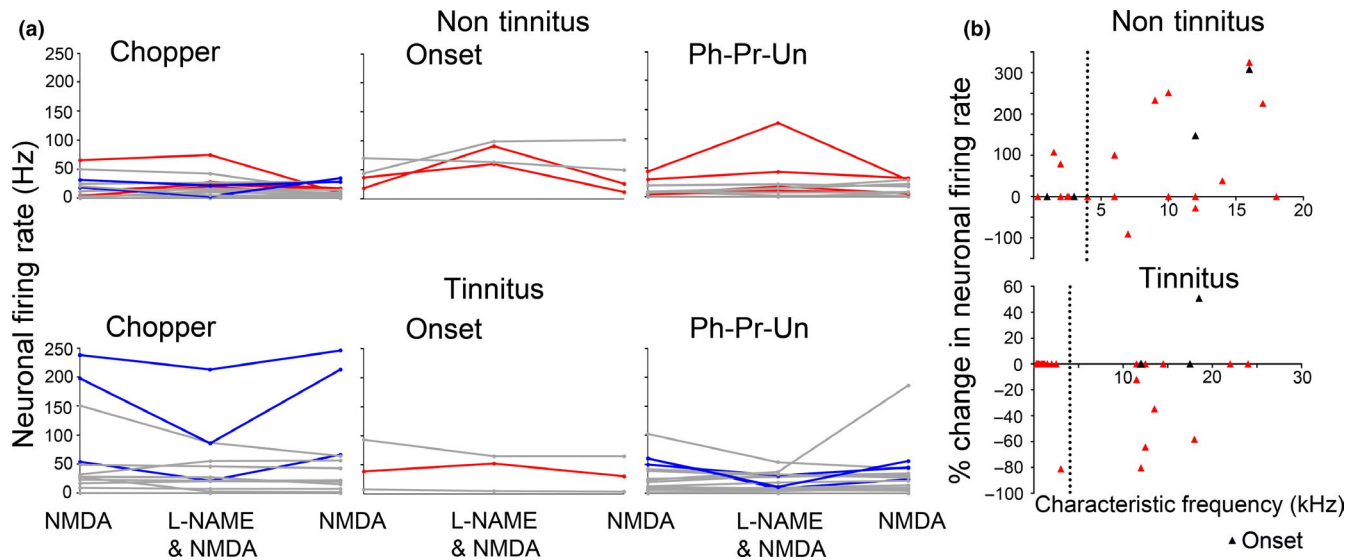
**FIGURE 11** (a) The percentage change of VCN units significantly increasing or decreasing their NMDA-evoked excitation during L-NAME application, for non-tinnitus and tinnitus groups and each neuronal class. The red lines show a significant increase in firing rate, while the blue lines show a significant decrease. Grey lines have no significant change related to the L-NAME application. (b) These panels plot the changes in firing rate against the characteristic frequency of the units. The vertical dotted lines show the borders between the units that were (to the right) or were not (to the left) in a region with an increase in audiometric threshold following the noise exposure. The black triangles represent onset units, and the red triangles represent all the other types of unit.

decrease in firing rate in response to the L-NAME. The only cell type to show an increase in response to L-NAME was an onset cell. The PSTHs of the units in the tinnitus group that showed an altered response to NMDA in the presence of L-NAME are shown in Figure S3.

The animals were all noise-exposed with a narrow-band noise centred at 9 kHz, and our estimates of hearing threshold indicated that there was little alteration among cells with CFs of 4 kHz or less. When CF was plotted against the change in NMDA-induced firing rate produced by L-NAME, very few cells with CFs of 4 kHz or below showed a significant change (two in the non-tinnitus group and one in the tinnitus group as determined by applying a Kruskal–Wallis test with Dunn's multiple comparison; Figure 11b). Most of the responsive units had CFs of 6–20 kHz and that was true of both the onset cells (black triangles) and other types. The main feature of these plots is that they illustrate the strong facilitation of responses in the non-tinnitus group and the suppression of responses in the tinnitus group.

# 4 | DISCUSSION

## 4.1 | Nitric oxide mediates increased gain in the VCN of animals with tinnitus

The main goal of this study was to test the hypothesis that increased levels of nitric oxide in the VCN contributed to the increased gain applied to input from the auditory nerve after the induction of tinnitus caused by unilateral noise exposure.

Previous work has shown that there is "increased central gain" present in tinnitus animals (Auerbach et al., 2014; Noreña, 2011). Maladaptive homeostatic plasticity in the cochlear nucleus may be the first step in a system of increased gain, whereby brainstem gain returns mean firing rates to long-term mean values, while simultaneously pathologically increasing spontaneous firing rates. Over-compensation of the gain control may produce driven activity in tinnitus animals that is also higher than that of controls, and this may be linked to hyperacusis (Chen et al., 2013), which has a high comorbidity with tinnitus (Roberts, 2018). In line with this, we have found evidence that, despite permanent threshold changes in all the noise-exposed animals, the driven firing rates of neurons in the VCN of tinnitus animals are maintained at similar levels to those seen in controls. By contrast, the mean driven firing rate of non-tinnitus animals is significantly reduced. When the production of endogenous NO was blocked with a NOS inhibitor, 37% of neurons in the tinnitus animals showed a reduction in driven firing rate, while in the non-tinnitus animals, it was only 5%. This shows that in the tinnitus animals, endogenous release of NO is facilitating the driven firing rate and maintaining it at control levels despite a reduced auditory input. NO does not have this function in non-tinnitus animals, and the driven firing rate of neurons in the VCN is less than controls. We have previously shown that there is a relative increase in nNOS staining in the VCN on the noise-exposed side of the brain (Coomber et al., 2014, 2015). This increase only appears to occur in animals that subsequently develop tinnitus. It did not occur in animals that had been noise-exposed but showed no behavioural evidence

of tinnitus 8 weeks later. Taken together, these results indicate that the increased nNOS expression is causally linked to the maintenance of driven firing rates in tinnitus animals.

Two recent studies have also provided evidence that NO is involved in a positive feedback mechanism in the VCN. It can act through interneurons that interconnect the chopper cells that project into the brainstem via the trapezoid body (T-stellates: Cao et al., 2019), but also affects the firing rate of primary-like bushy cells and the large stellates with onset properties (Hockley et al., 2020). In the control VCN, only about a quarter of neurons express detectable levels of nNOS (Coomber et al., 2015) and similar numbers of neurons appear to be susceptible to modification of their firing rate by altered NO levels (Hockley et al., 2020). However, in the current study, after AOE, the percentage of neurons that respond to an exogenous source of NO was more than doubled.

In the tinnitus animals, the spontaneous firing rates also increased compared with the control animals, while there was no significant change in the non-tinnitus animals. This study is the first to show a correlation between behavioural evidence of tinnitus and increased spontaneous rates in the VCN, and this contrasts with the lack of behaviourally specific increases that have been found in the inferior colliculus (Coomber et al., 2014; Longenecker & Galazyuk, 2016; Ropp, Tiedemann, Young, & May, 2014). A recent study has also shown changes in voltage-dependent potassium channels, which occur after deafferentation of the cochlea, and are present in the VCN, but not higher up the auditory pathway in the inferior colliculus (Poveda et al., 2020). Previously, it has been shown that noise exposure produces hyperactivity in VCN slices immediately after AOE (Gröschel, Ryll, Gotze, Ernst, & Basta, 2014). Changes have also been shown in the VCN in vivo following cochlear trauma, with hyperactivity occurring as a result of intense AOE or mechanical lesion (Vogler, Robertson, & Mulders, 2011). A further study showed that this VCN hyperactivity was due to increased activity in primary-like and onset neurons (Robertson, Bester, Vogler, & Mulders, 2013). The present study did not observe any correlation between significant increases in spontaneous rate and any specific neuronal subtype, but this may just have been because of our relatively small samples. There was an increase in the number of units where blocking NOS caused a decrease in spontaneous firing rate of neurons in the tinnitus animals, but this was also true of the non-tinnitus animals and in neither case was there a significant difference from the controls. Thus, we were unable to show that the increased spontaneous rate was due to an increase in the amount of endogenous NO release. Increased spontaneous activity at various points on the auditory pathway appears to be associated with the presence of tinnitus (Shore & Wu, 2019), but there was no evidence of a direct link between increased NO release in the VCN and increased spontaneous activity. Such a link may still exist as NO-induced increases in cGMP

levels have been shown to modify spontaneous firing rate of Purkinje cells in the cerebellum (Smith & Otis, 2003). NO production may be involved in the development of tinnitus, and other studies give indications of how it might be acting.

## 4.2 | Potential role of NO in the VCN during the development of tinnitus

The neural mechanisms underlying tinnitus are still not fully understood (Shore et al., 2016). Tinnitus is a conscious experience that is linked to stress levels, and as such, it is thought to involve parts of the auditory cortex and the limbic system (Sedley, 2019). Despite this, there is increasingly strong evidence from animal models that the cochlear nucleus is involved in and may be essential for tinnitus development and maintenance (Shore & Wu, 2019). Most of the evidence is based on the dorsal cochlear nucleus where increasingly, detailed mechanisms of the plastic changes that may be involved in tinnitus have been described (Heeringa et al., 2018; Marks et al., 2018). These studies have been focussed on mechanisms for homeostatic plasticity, but an alternative mechanism for tinnitus development involves stochastic resonance where a reduced peripheral input is compensated for by a feedback system that increases internal noise (Gollnast et al., 2017). Our demonstration of increased spontaneous firing rates in the VCN, following noise exposure, is consistent with a role of VCN in stochastic resonance. Modelling work suggests that the internal noise associated with stochastic resonance could be applied to the DCN (Krauss et al., 2016) and one source for this input might be the VCN. The ventral and dorsal divisions of the cochlear nucleus are reciprocally connected (Cant & Benson, 2003) so that changes in their activity are mutually dependent. The VCN is also thought to be involved in tinnitus (Gu et al., 2012) and could be involved through a variety of output pathways one of which is to the DCN. Following the induction of tinnitus, there is a reduction in the number of glycine receptors in the DCN (Wang et al., 2009). This would affect one of the main glycinergic inputs to the DCN, which is from the large, D-stellate onset cells of the VCN (Arnott, Wallace, Shackleton, & Palmer, 2004). These neurons contain nNOS (Coomber et al., 2015), and the levels of nNOS seem to increase in tinnitus animals. One of the actions of NO is to act postsynaptically to reduce glycinergic inhibition via a cGMP-dependent mechanism for changing the inhibitory reversal potential by suppressing the potassium chloride co-transporter (Yassin et al., 2014). Thus, one way in which increased nNOS expression in the VCN might affect the development of tinnitus is through reduced inhibition of the DCN. The T-stellate, chopper cells also contain nNOS (Coomber et al., 2015) and project to the DCN (Oertel, Wright, Cao, Ferragamo, & Bal, 2011; Palmer, Wallace, Arnott, & Shackleton, 2003) to provide another direct route for the VCN to modulate activity in the DCN.

## 4.3 | NO mechanisms in the VCN of animals with tinnitus

The mechanisms by which NO can affect neural activity are many and varied, but the most important involves the activation of soluble guanylyl cyclase and the formation of cGMP, which acts through a protein kinase to phosphorylate a number of targets (Garthwaite, 2019). These targets include postsynaptic receptors and membrane channels (Steinert et al., 2011). A major route for producing NO involves the activation of NMDA receptors, which are located in the postsynaptic membrane and closely bound to nNOS and guanylyl cyclase in a multi-protein complex present as discrete puncta in the central nucleus of the IC (Olthof-Bakker et al., 2019). Similar discrete puncta of nNOS staining have been described in the VCN (Coomber et al., 2015), and they become more prominent following cochleostomy (Chen et al., 2004). These puncta may also represent the same type of multi-protein complex as is found in the IC. NMDA receptors are present in the VCN (Chen et al., 2004; Watanabe, Mishina, & Inoue, 1994), and different cell types have different sensitivities. The amplitude of EPSCs induced by NMDA is largest in T-stellates, smaller in bushy cells and smallest in octopus cells (Cao & Oertel, 2010). Activation of the NMDA channel leads to a localised influx of $Ca^{2+}$ ions to stimulate NO production and the production of cGMP, which can then inhibit the NMDA receptors via a feedback mechanism (Manzoni et al., 1992; Steinert et al., 2008). This feedback mechanism might explain why some neurons in both the control (Hockley et al., 2020) and non-tinnitus animals showed an enhanced response to sound or NMDA when L-NAME was present. However, in the tinnitus group significantly increased numbers of neurons showed the opposite effect where blocking NO production with L-NAME reduced the driven firing rate or response to NMDA. This result would require a different mechanism. It suggests that the elevated NO levels may not be producing a negative feedback effect on the NMDA receptors and this lack of an effect has already been described in neurons of the rat hippocampus (Hopper, Lancaster, & Garthwaite, 2004). Instead, different targets may be affected by the cGMP-activated protein kinase (PKG). We were able to show that in the tinnitus animals, 25% (11/44) of neurons where NO levels were manipulated showed a change in the width of their action potential, whereas in the control group, this figure was 2% (2/94: Hockley et al., 2020). This indicates that the function of NO has changed after noise exposure and in vivo studies of a different neuronal system (cat visual cortex) have already shown that blocking the activity of NOS can reduce the responses to both sensory stimulation and the application of NMDA (Cudeiro et al., 1997).

## 4.4 | Nitric oxide pathways as a therapeutic target for treating tinnitus

Our results provide further evidence that changes in the function of NO in the VCN may be involved in the development of tinnitus. This leads on to the question of whether some part of the regulatory pathway involving NO may provide a therapeutic target to interfere with the initial production or even maintenance of tinnitus. NO itself is produced by neurons in almost all parts of the brain and peripheral nervous system (Vincent & Kimura, 1992), but nNOS itself is too widespread a target in the brain to be suitable for treating a specific problem such as tinnitus. One potential alternative is to target the peripheral processes that lead to changes in NO production. NO production has already been established as a potential therapeutic target in reducing neuropathic pain, a condition often likened to tinnitus (Flores et al., 2015; Tonndorf, 1987) due to the similarities of increased central gain following peripheral damage (Cury, Picolo, Gutierrez, & Ferreira, 2011). The spiral ganglion neurons contain relatively high levels of nNOS (Riemann & Reuss, 1999) and are known to slowly degenerate following noise exposure (Lin, Furman, Kujawa, & Liberman, 2011). This degeneration is associated with the release of inflammatory mediators and increased levels of nNOS (Heinrich & Helling, 2012). Circulating glucocorticoids associated with increased stress also increase the NO production in the auditory nerve (Yukawa, Shen, Harada, Cho-Tamaoka, & Yamashita, 2005). Any increase in NO levels can change the kinetics of HCN channels that regulate the excitability and resting membrane potential of neurons (Kopp-Scheinpflug, Pigott, & Forsythe, 2015). The auditory nerve is not thought to contain significant levels of guanylyl cyclase (Burette, Petrusz, Schmidt, & Weinberg, 2001), but NO can activate HCN channels in neurons through a cGMP-independent mechanism (Wenker et al., 2012). These channels may then increase the level of spontaneous activity in the auditory nerve. Neuropathic pain is also thought to be caused by increased levels of spontaneous activity in small peripheral nerve fibres due to increased activity in HCN2 channels. Blocking these channels can block the neuropathic pain (Tsantoulas, Mooney, & McNaughton, 2016), and we are currently investigating whether blocking peripheral HCN channels might have an effect on tinnitus as well.

An alternative target is the second messenger (cGMP) that NO usually acts through. The cGMP levels are a product of the rate of production by guanylyl cyclase minus the rate of inactivation by phosphodiesterases (PDEs). Guanylyl cyclase is found in all the principal neurons of the VCN (Burette et al., 2001). There are 11 different types of PDE, and they are increasingly becoming therapeutic targets in a variety of diseases involving NO production (Maurice

et al., 2014). Only a subset of them will be found in the auditory system, but already drug trials with PDE5 inhibitors have been carried out to treat tinnitus in humans (Mazurek et al., 2009), or following blast exposure in rats (Mahmood et al., 2014). However, these have had limited success, potentially because PDE5 may be more common in other parts of the brain and periphery than in the auditory system. To be effective, a drug like a PDE inhibitor ought to be more specific for the parts of the brain thought to be involved in tinnitus (Shore & Wu, 2019). Some forms of PDE such as PDE2A have been identified in fibres of the cochlear nucleus of rats. Although it is also found in many other parts of the brain (Stephenson et al., 2009), these include the hippocampus and other parts of the limbic system that may also have a role in the stress associated with severe tinnitus (Eggermont & Roberts, 2015). Thus, PDE2 might be a potential target for treating tinnitus, as blocking it can produce increased levels of cGMP in target neurons and these could include neurons in the cochlear nucleus. A secondary effect would be to act as an anxiolytic for treating any anxiety associated with the tinnitus (Masood et al., 2009).

## CONFLICT OF INTEREST
The authors declare that the research was conducted in the absence of any commercial or financial relationships that could be construed as a potential conflict of interest.

## AUTHOR CONTRIBUTIONS
AH, MNW and ARP conceived the experimental ideas and design; AH collected all the physiological data with the help of ARP; AH analysed the data with the help of JIB and MNW; AH and MNW wrote the manuscript and prepared the figures, while JIB and ARP reviewed and edited the manuscript.

## DATA AVAILABILITY STATEMENT
The original data files are available by contacting the first or last authors.

## PEER REVIEW
The peer review history for this article is available at https://publons.com/publon/10.1111/ejn.14913

## ORCID
*Joel I. Berger* https://orcid.org/0000-0002-1960-9487
*Mark N. Wallace* https://orcid.org/0000-0001-6894-4903

## REFERENCES
Alvarado, J. C., Fuentes-Santamaría, V., Gabaldón-Ull, M. C., Jareño-Flores, T., Miller, J. M., & Juiz, J. M. (2016). Noise-induced "toughening" effect in Wistar rats: Enhanced auditory brainstem responses are related to calretinin and nitric oxide synthase upregulation. *Frontiers in Neuroanatomy*, *10*, 1–24. https://doi.org/10.3389/fnana.2016.00019

Arnott, R. H., Wallace, M. N., Shackleton, T. M., & Palmer, A. R. (2004). Onset neurons in the anteroventral cochlear nucleus project to the dorsal cochlear nucleus. *Journal of the Association for Research in Otolaryngology*, *5*, 1153–1170.

Auerbach, B. D., Rodrigues, P. V., Salvi, R. J., Zhang, J., Shaikh, A. G., & Liu, B. (2014). Central gain control in tinnitus and hyperacusis. *Frontiers in Neurology*, *5*, 1–21. https://doi.org/10.3389/fneur.2014.00206

Berger, J. I., Coomber, B., Shackleton, T. M., Palmer, A. R., & Wallace, M. N. (2013). A novel behavioural approach to detecting tinnitus in the guinea pig. *Journal of Neuroscience Methods*, *213*, 188–195. https://doi.org/10.1016/j.jneumeth.2012.12.023

Berger, J. I., Coomber, B., Wallace, M. N., & Palmer, A. R. (2016). Reductions in cortical alpha activity, enhancements in neural responses and impaired gap detection caused by sodium salicylate in awake guinea pigs. *European Journal of Neuroscience*, *45*, 398–409. https://doi.org/10.1111/ejn.13474

Berger, J. I., Coomber, B., Wells, T. T., Wallace, M. N., & Palmer, A. R. (2014). Changes in the response properties of inferior colliculus neurons relating to tinnitus. *Frontiers in Neurology*, *5*, 203. https://doi.org/10.3389/fneur.2014.00203

Berger, J. I., Owen, W., Wilson, C. A., Hockley, A., Coomber, B., Palmer, A. R., & Wallace, M. N. (2018). Gap-induced reductions of evoked potentials in the auditory cortex: A possible objective marker for the presence of tinnitus in animals. *Brain Research*, *1679*, 101–108. https://doi.org/10.1016/j.brainres.2017.11.026

Bullock, D. C., Palmer, A. R., & Rees, A. (1988). Compact and easy-to-use tungsten-in-glass microelectrode manufacturing workstation. *Medical and Biological Engineering & Computing*, *26*, 669–672. https://doi.org/10.1007/BF02447511

Burette, A., Petrusz, P., Schmidt, H. H., & Weinberg, R. J. (2001). Immunohistochemical localization of nitric oxide synthase and soluble guanylyl cyclase in the ventral cochlear nucleus of the rat. *The Journal of Comparative Neurology*, *431*, 1–10. https://doi.org/10.1002/1096-9861(20010226)431:1<1:AID-CNE1051>3.0.CO;2-E

Cant, N. B., & Benson, C. G. (2003). Parallel auditory pathways: Projection patterns of the different neuronal populations in the dorsal and ventral cochlear nuclei. *Brain Research Bulletin*, *60*, 457–474. https://doi.org/10.1016/S0361-9230(03)00050-9

Cao, X. J., Lin, L., Sugden, A. U., Connors, B. W., & Oertel, D. (2019). Nitric oxide-mediated plasticity of interconnections between T-stellate cells of the ventral cochlear nucleus generate positive feedback and constitute a central gain control in the auditory system. *The Journal of Neuroscience*, *39*, 6095–6107. https://doi.org/10.1523/JNEUROSCI.0177-19.2019

Cao, X.-J., & Oertel, D. (2010). Auditory nerve fibers excite targets through synapses that vary in convergence, strength, and short-term

plasticity. *Journal of Neurophysiology*, *104*, 2308–2320. https://doi.org/10.1152/jn.00451.2010

Chen, G., Lee, C., Sandridge, S. A., Butler, H. M., Manzoor, N. F., & Kaltenbach, J. A. (2013). Behavioral evidence for possible simultaneous induction of hyperacusis and tinnitus following intense sound exposure. *Journal of the Association for Research in Otolaryngology*, *14*, 413–424. https://doi.org/10.1007/s10162-013-0375-2

Chen, T. J., Huang, C. W., Wang, D. C., & Chen, S. S. (2004). Co-induction of growth-associated protein GAP-43 and neuronal nitric oxide synthase in the cochlear nucleus following cochleotomy. *Experimental Brain Research*, *158*, 151–162. https://doi.org/10.1007/s00221-004-1886-1

Christopherson, K. S., Hillier, B. J., Lim, W. A., & Bredt, D. S. (1999). PSD95 assembles a ternary complex with the N-methyl-D-aspartic acid receptor and a bivalent neuronal NO synthase PDZ domain. *Journal of Biological Chemistry*, *274*, 27467–27473.

Coomber, B., Berger, J. I., Kowalkowski, V. L., Shackleton, T. M., Palmer, A. R., & Wallace, M. N. (2014). Neural changes accompanying tinnitus following unilateral acoustic trauma in the guinea pig. *European Journal of Neuroscience*, *40*, 2427–2441. https://doi.org/10.1111/ejn.12580

Coomber, B., Kowalkowski, V. L., Berger, J. I., Palmer, A. R., & Wallace, M. N. (2015). Modulating central gain in tinnitus: Changes in nitric oxide synthase in the ventral cochlear nucleus. *Frontiers in Neurology*, *6*, 1–12. https://doi.org/10.3389/fneur.2015.00053

Cudeiro, J., Rivadulla, C., Rodriguez, R., Grieve, K., Martinez-Conde, S., & Acuna, C. (1997). Actions of compounds manipulating the nitric oxide system in the cat primary visual cortex. *Journal of Physiology*, *504*, 467–478. https://doi.org/10.1111/j.1469-7793.1997.467be.x

Cury, Y., Picolo, G., Gutierrez, V. P., & Ferreira, S. H. (2011). Pain and analgesia: The dual effect of nitric oxide in the nociceptive system. *Nitric Oxide - Biology and Chemistry*, *25*, 243–254. https://doi.org/10.1016/j.niox.2011.06.004

Dehmel, S., Eisinger, D., & Shore, S. E. (2012). Gap prepulse inhibition and auditory brainstem evoked potentials as objective measures for tinnitus in guinea pigs. *Frontiers in Systems Neuroscience*, *6*, 42. https://doi.org/10.3389/fnsys.2012.00042

Dong, S., Mulders, W. H. A. M., Rodger, J., & Robertson, D. (2009). Changes in neuronal activity and gene expression in guinea-pig auditory brainstem after unilateral partial hearing loss. *Neuroscience*, *159*, 1164–1174. https://doi.org/10.1016/j.neuroscience.2009.01.043

Dong, S., Mulders, W. H. A. M., Rodger, J., Woo, S., & Robertson, D. (2010). Acoustic trauma evokes hyperactivity and changes in gene expression in guinea-pig auditory brainstem. *European Journal of Neuroscience*, *31*, 1616–1628. https://doi.org/10.1111/j.1460-9568.2010.07183.x

Eggermont, J. J. (2015). Tinnitus and neural plasticity (Tonndorf lecture at XIth International Tinnitus Seminar, Berlin, 2014). *Hearing Research*, *319*, 1–11. https://doi.org/10.1016/j.heares.2014.10.002

Eggermont, J. J., & Roberts, L. E. (2015). Tinnitus: Animal models and findings in humans. *Cell Tissue Research*, *361*, 311–336. https://doi.org/10.1007/s00441-014-1992-8

Flores, E. N., Duggan, A., Madathany, T., Hogan, A. K., Márquez, F. G., Kumar, G., … García-Añoveros, J. (2015). A non-canonical pathway from cochlea to brain signals tissue-damaging noise. *Current Biology*, *25*, 606–612. https://doi.org/10.1016/j.cub.2015.01.009

Fournier, P., & Hebert, S. (2013). Gap detection deficits in humans with tinnitus as assessed with the acoustic startle paradigm: Does tinnitus fill in the gap? *Hearing Research*, *295*, 16–23. https://doi.org/10.1016/j.heares.2012.05.011

Freeman, G. H., & Halton, J. H. (1951). Note on exact treatment of contingency, goodness of fit and other problems of significance. *Biometrika*, *38*, 141–149.

Garthwaite, J. (2019). NO as a multimodal transmitter in the brain: Discovery and current status. *British Journal of Pharmacology*, *176*, 197–211. https://doi.org/10.1111/bph.14532

Gollnast, D., Tziridis, K., Krauss, P., Schilling, A., Hoppe, U., & Schulze, H. (2017). Analysis of audiometric differences of patients with and without tinnitus in a large clinical database. *Frontiers in Neurology*, *8*, 31. https://doi.org/10.3389/fneur.2017.00031

Gröschel, M., Ryll, J., Gotze, R., Ernst, A., & Basta, D. (2014). Acute and long-term effects of noise exposure on the neuronal spontaneous activity in cochlear nucleus and inferior colliculus brain slices. *BioMed Research International*, *2014*, 909160. https://doi.org/10.1155/2014/909260

Gu, J. W., Herrmann, B. S., Levine, R. A., & Melcher, J. R. (2012). Brainstem auditory evoked potentials suggest a role for the ventral cochlear nucleus in tinnitus. *Journal of the Association for Research in Otolaryngology*, *13*, 819–833. https://doi.org/10.1007/s10162-012-0344-1

Heeringa, A. N., Wu, C., Chung, C., West, M., Martel, D., Liberman, L., … Shore, S. E. (2018). Glutamatergic projections to the cochlear nucleus are redistributed in tinnitus. *Neuroscience*, *391*, 91–103. https://doi.org/10.1016/j.neuroscience.2018.09.008

Heinrich, U.-R., & Helling, K. (2012). Nitric oxide—A versatile key player in cochlear function and hearing disorders. *Nitric Oxide*, *27*, 106–116. https://doi.org/10.1016/j.niox.2012.05.005

Hockley, A., Berger, J. I., Smith, P. A., Palmer, P. A., & Wallace, M. N. (2020). Nitric oxide regulates the firing rate of neuronal subtypes in the guinea pig ventral cochlear nucleus. *European Journal of Neuroscience*, *51*, 963–983. https://doi.org/10.1111/ejn.14572

Hollas, M. A., Ben Aissa, M., Lee, S. H., Gordon-Blake, J. M., & Thatcher, G. R. J. (2019). Pharmacological manipulation of cGMP and NO/cGMP in CNS drug discovery. *Nitric Oxide*, *82*, 59–74. https://doi.org/10.1016/j.niox.2018.10.006

Hopper, R., Lancaster, B., & Garthwaite, J. (2004). On the regulation of NMDA receptors by nitric oxide. *European Journal of Neuroscience*, *19*, 1675–1682. https://doi.org/10.1111/j.1460-9568.2004.03306.x

Johnstone, J. R., Alder, V. A., Johnstone, B. M., Robertson, D., & Yates, Y. K. (1979). Cochlear action potential threshold and single unit thresholds. *Journal of the Acoustical Society of America*, *65*, 254–257. https://doi.org/10.1121/1.382244

Knowles, R. G., & Moncada, S. (1994). Nitric oxide synthases in mammals. *Biochemistry Journal*, *298*, 249–258. https://doi.org/10.1042/bj2980249

Koerber, K. C., Pfeiffer, R. R., Warr, W. B., & Kiang, N. Y. S. (1966). Spontaneous spike discharges from single units in the cochlear nucleus after destruction of the cochlea. *Experimental Neurology*, *16*, 119–130. https://doi.org/10.1016/0014-4886(66)90091-4

Kopp-Scheinpflug, C., Pigott, B. M., & Forsythe, I. D. (2015). Nitric oxide selectively suppresses IH currents mediated by HCN1-containing channels. *Journal of Physiology*, *593*, 1685–1700.

Krauss, P., Tziridis, K., Metzner, C., Schilling, A., Hoppe, U., & Schulze, H. (2016). Stochastic resonance controlled upregulation of internal noise after hearing loss as a putative cause of tinnitus-related

neuronal hyperactivity. *Frontiers in Neuroscience*, *10*, 597. https://doi.org/10.3389/fnins.2016.00597

Lin, H. W., Furman, A. C., Kujawa, S. G., & Liberman, M. C. (2011). Primary neural degeneration in the guinea pig cochlea after reversible noise-induced threshold shift. *Journal of the Association for Research in Otolaryngology*, *12*, 605–616. https://doi.org/10.1007/s10162-011-0277-0

Longenecker, R. J., & Galazyuk, A. V. (2011). Development of tinnitus in CBA/CaJ mice following sound exposure. *Journal of the Association for Research in Otolaryngology*, *12*, 647–658. https://doi.org/10.1007/s10162-011-0276-1

Longenecker, R. J., & Galazyuk, A. V. (2016). Variable effects of acoustic trauma on behavioral and neural correlates of tinnitus in individual animals. *Frontiers in Behavioral Neuroscience*, *10*, 207. https://doi.org/10.3389/fnbeh.2016.00207

Mahmood, G., Mei, Z., Hojjat, H., Pace, E., Kallakuri, S., & Zhang, J. S. (2014). Therapeutic effect of sildenafil on blast-induced tinnitus and auditory impairment. *Neuroscience*, *269*, 367–382. https://doi.org/10.1016/j.neuroscience.2014.03.020

Manzoni, O., Prezeau, L., Marin, P., Desagher, S., Bockaert, J., & Fagni, L. (1992). Nitric oxide-induced blockade of NMDA receptors. *Neuron*, *8*, 653–662. https://doi.org/10.1016/0896-6273(92)90087-T

Marks, K. L., Martel, D. T., Wu, C., Basura, G. J., Roberts, L. E., Schvartz-Leyzac, K. C., & Shore, S. E. (2018). Auditory-somatosensory bimodal stimulation desynchronizes brain circuitry to reduce tinnitus in guinea pigs and humans. *Science Translational Medicine*, *10*(422), eaal3175. https://doi.org/10.1126/scitranslmed.aal3175

Masood, A., Huang, Y., Hajjhussein, H., Xiao, L., Li, H., Wang, W., … O'Donnell, J. M. (2009). Anxiolytic effects of phosphodiesterase-2 inhibitors associated with increased cGMP signaling. *The Journal of Pharmacology and Experimental Therapeutics*, *331*, 690–699. https://doi.org/10.1124/jpet.109.156729

Maurice, D. H., Ke, H., Ahmad, F., Wang, Y., Chung, J., & Manganiello, V. C. (2014). Advances in targeting cyclic nucleotide phosphodiesterases. *Nature Reviews of Drug Discovery*, *13*, 290–314. https://doi.org/10.1038/nrd4228

Mazurek, B., Haupt, H., Szczepek, A. J., Sandmann, J., Gross, J., Klapp, B. F., … Caffier, P. P. (2009). Evaluation of vardenafil for the treatment of subjective tinnitus: A controlled pilot study. *Journal of Negative Results in Biomedicine*, *8*, 3. https://doi.org/10.1186/1477-5751-8-3

Noreña, A. J. (2011). An integrative model of tinnitus based on a central gain controlling neural sensitivity. *Neuroscience and Biobehavioral Reviews*, *35*, 1089–1109. https://doi.org/10.1016/j.neubiorev.2010.11.003

Oertel, D., Wright, S., Cao, X. J., Ferragamo, M., & Bal, R. (2011). The multiple functions of T stellate/multipolar/chopper cells in the ventral cochlear nucleus. *Hearing Research*, *276*, 61–69. https://doi.org/10.1016/j.heares.2010.10.018

Olthof-Bakker, B. M. J., Gartside, S. E., & Rees, A. (2019). Puncta of neuronal nitric oxide synthase (nNOS) mediate NMDA-receptor signalling in the auditory midbrain. *Journal of Neuroscience*, *39*, 876–887.

Palmer, A. R., & Shackleton, T. M. (2009). Variation in the phase of response to low-frequency pure tones in the guinea pig auditory nerve as functions of stimulus level and frequency. *Journal of the Association for Research in Otolaryngology*, *10*, 233–250. https://doi.org/10.1007/s10162-008-0151-x

Palmer, A. R., Wallace, M. N., Arnott, R. H., & Shackleton, T. M. (2003). Morphology of physiologically characterised ventral cochlear nucleus stellate cells. *Experimental Brain Research*, *153*, 418–426. https://doi.org/10.1007/s00221-003-1602-6

Poveda, C. M., Valero, M. L., Pernia, M., Alvara, J. C., Ryugo, D. K., Merchan, M. A., & Juiz, J. M. (2020). Expression and localization of Kv1.1 and Kv3.1b potassium channels in the cochlear nucleus and inferior colliculus after long-term auditory deafferentation. *Brain Sciences*, *10*, 35. https://doi.org/10.3390/brainsci10010035

Prast, H., & Philippu, A. (2001). Nitric oxide as modulator of neuronal function. *Progress in Neurobiology*, *64*, 51–68. https://doi.org/10.1016/S0301-0082(00)00044-7

Riemann, R., & Reuss, S. (1999). Nitric oxide synthase in identified olivocochlear projection neurons in rat and guinea pig. *Hearing Research*, *135*, 181–189. https://doi.org/10.1016/S0378-5955(99)00113-6

Roberts, L. E. (2018). Neural plasticity and its initiating conditions in tinnitus. *HNO*, *66*, 172–178. https://doi.org/10.1007/s00106-017-0449-2

Robertson, D., Bester, C., Vogler, D., & Mulders, W. H. A. M. (2013). Spontaneous hyperactivity in the auditory midbrain: Relationship to afferent input. *Hearing Research*, *295*, 124–129. https://doi.org/10.1016/j.heares.2012.02.002

Ropp, T.-J.-F., Tiedemann, K. L., Young, E. D., & May, B. J. (2014). Effects of unilateral acoustic trauma on tinnitus-related spontaneous activity in the inferior colliculus. *Journal of the Association for Research in Otolaryngology*, *15*, 1007–1022. https://doi.org/10.1007/s10162-014-0488-2

Schaette, R., & McAlpine, D. (2011). Tinnitus with a normal audiogram: Physiological evidence for hidden hearing loss and computational model. *Journal of Neuroscience*, *31*, 13452–13457. https://doi.org/10.1523/JNEUROSCI.2156-11.2011

Schilling, A., Krauss, P., Gerum, R., Metzner, C., Tziridis, K., & Schulze, H. (2017). A new statistical approach for the evaluation of gap-prepulse inhibition of the acoustic startle reflex (GPIAS) for tinnitus assessment. *Frontiers in Behavioral Neuroscience*, *11*, 198. https://doi.org/10.3389/fnbeh.2017.00198

Schofield, B. R., & Cant, N. B. (1996). Origins and targets of commissural connections between the cochlear nuclei in guinea pigs. *Journal of Comparative Neurology*, *375*, 128–146. https://doi.org/10.1002/(SICI)1096-9861(19961104)375:1<128:AID-CNE8>3.0.CO;2-5

Sedley, W. (2019). Tinnitus: Does gain explain? *Neuroscience*, *407*, 213–228. https://doi.org/10.1016/j.neuroscience.2019.01.027

Sheppard, A., Liu, X., Ding, D., & Salvi, R. J. (2018). Auditory central gain compensates for changes in cochlear output after prolonged low-level noise exposure. *Neuroscience Letters*, *687*, 183–188. https://doi.org/10.1016/j.neulet.2018.09.054

Shore, S. E., Roberts, L. E., & Langguth, B. (2016). Maladaptive plasticity in tinnitus—Triggers, mechanisms and treatment. *Nature Reviews Neurology*, *12*, 150–160. https://doi.org/10.1038/nrneurol.2016.12

Shore, S. E., & Wu, C. (2019). Mechanisms of noise-induced tinnitus: Insights from cellular studies. *Neuron*, *103*, 8–20. https://doi.org/10.1016/j.neuron.2019.05.008

Smith, S. L., & Otis, T. S. (2003). Persistent changes in spontaneous firing of Purkinje neurons triggered by the nitric oxide signaling cascade. *Journal of Neuroscience*, *23*, 367–372. https://doi.org/10.1523/JNEUROSCI.23-02-00367.2003

Steinert, J. R., Kopp-Scheinpflug, C., Baker, C., Challiss, R. A. J., Mistry, R., Haustein, M. D., … Forsythe, I. D. (2008). Nitric oxide is a volume transmitter regulating postsynaptic excitability at a glutamatergic synapse. *Neuron*, *60*, 642–656. https://doi.org/10.1016/j.neuron.2008.08.025

Steinert, J. R., Robinson, S. W., Tong, H., Haustein, M. D., Kopp-Scheinpflug, C., & Forsythe, I. D. (2011). Nitric oxide is an activity-dependent regulator of target neuron intrinsic excitability. *Neuron*, *71*, 291–305. https://doi.org/10.1016/j.neuron.2011.05.037

Stephenson, D. T., Coskran, T. M., Wilhelms, M. B., Adamowicz, W. O., O'Donnell, M. M., Muravnick, K. B., … Morton, D. (2009). Immunohistochemical localization of phosphodiesterase 2A in multiple mammalian species. *Journal of Histochemistry and Cytochemistry*, *57*, 933–949. https://doi.org/10.1369/jhc.2009.953471

Sumner, C. J., Tucci, D. L., & Shore, S. E. (2005). Responses of ventral cochlear nucleus neurons to contralateral sound after conductive hearing loss. *Journal of Neurophysiology*, *94*, 4234–4243. https://doi.org/10.1152/jn.00401.2005

Tonndorf, J. (1987). The analogy between tinnitus and pain: A suggestion for a physiological basis of chronic tinnitus. *Hearing Research*, *28*, 271–275. https://doi.org/10.1016/0378-5955(87)90054-2

Tsantoulas, C., Mooney, E. R., & McNaughton, P. A. (2016). HCN2 ion channels: Basic science opens up possibilities for therapeutic intervention in neuropathic pain. *Biochemical Journal*, *473*, 2717–2736. https://doi.org/10.1042/BCJ20160287

Turner, J. G., Brozoski, T. J., Bauer, C. A., Parrish, J. L., Myers, K., Hughes, L. F., & Caspary, D. M. (2006). Gap detection deficits in rats with tinnitus: A potential novel screening tool. *Behavioral Neuroscience*, *120*, 188–195. https://doi.org/10.1037/0735-7044.120.1.188

Turner, J., Larsen, D., Hughes, L., Moechars, D., & Shore, S. E. (2012). Time course of tinnitus development following noise exposure in mice. *Journal of Neuroscience Research*, *90*, 1480–1488. https://doi.org/10.1002/jnr.22827

Turner, J. G., & Parrish, J. L. (2008). Gap detection methods for assessing salicylate-induced tinnitus and hyperacusis in rats. *American Journal of Audiology*, *17*, S185–S192. https://doi.org/10.1044/1059-0889(2008/08-0006)

Turrigiano, G. (1999). Homeostatic plasticity in neuronal networks: The more things change, the more they stay the same. *Trends in Neuroscience*, *22*, 221–227. https://doi.org/10.1016/S0166-2236(98)01341-1

Vincent, S. R., & Kimura, H. (1992). Histochemical mapping of nitric oxide synthase in the rat brain. *Neuroscience*, *46*, 755–784. https://doi.org/10.1016/0306-4522(92)90184-4

Vogler, D. P., Robertson, D., & Mulders, W. H. A. M. (2011). Hyperactivity in the ventral cochlear nucleus after cochlear trauma. *The Journal of Neuroscience*, *31*, 6639–6645. https://doi.org/10.1523/JNEUROSCI.6538-10.2011

Wang, H., Brozoski, T. J., Turner, J. G., Ling, L., Parrish, J. L., Hughes, L. F., & Caspary, D. M. (2009). Plasticity at glycinergic synapses in dorsal cochlear nucleus of rats with behavioral evidence of tinnitus. *Neuroscience*, *164*, 747–759. https://doi.org/10.1016/j.neuroscience.2009.08.026

Watanabe, M., Mishina, M., & Inoue, Y. (1994). Distinct distributions of five NMDA receptor channel subunit mRNAs in the brainstem. *The Journal of Comparative Neurology*, *343*, 520–531. https://doi.org/10.1002/cne.903430403

Wenker, I. C., Benoit, J. P., Chen, X., Liu, H., Horner, R. L., & Mulkey, D. K. (2012). Nitric oxide activates hypoglossal motoneurons by cGMP-dependent inhibition of TASK channels and cGMP-independent activation of HCN channels. *Journal of Neurophysiology*, *107*, 1489–1499. https://doi.org/10.1152/jn.00827.2011

Yassin, L., Radtke-Schuller, S., Asraf, H., Grothe, B., Hershfinkel, M., Forsythe, I. D., & Kopp-Scheinpflug, C. (2014). Nitric oxide signaling modulates synaptic inhibition in the superior paraolivary (SPN) via cGMP-dependent suppression of KCC2. *Frontiers in Neural Circuits*, *8*, 1–12.

Yukawa, H., Shen, J., Harada, N., Cho-Tamaoka, H., & Yamashita, T. (2005). Acute effects of glucocorticoids on ATP-induced Ca2+ mobilization and nitric oxide production in cochlear spiral ganglion neurons. *Neuroscience*, *130*, 485–496. https://doi.org/10.1016/j.neuroscience.2004.09.037

Zheng, Y., Seung Lee, H., Smith, P. F., & Darlington, C. L. (2006). Neuronal nitric oxide synthase expression in the cochlear nucleus in a salicylate model of tinnitus. *Brain Research*, *1123*, 201–206. https://doi.org/10.1016/j.brainres.2006.09.045

## SUPPORTING INFORMATION

Additional supporting information may be found online in the Supporting Information section.